Identification of a novel antigen-presenting cell population modulating antiinfluenza type 2 immunity

Jae-Kwang Yoo,[1,2] Carole L. Galligan,[1,2] Carl Virtanen,[3] and Eleanor N. Fish[1,2]

[1]Toronto General Research Institute, University Health Network, Toronto, Ontario M5G 2M1, Canada
[2]Department of Immunology, University of Toronto, Toronto, Ontario M5S 1A8, Canada
[3]Microarray Centre, University Health Network, Toronto, Ontario M5G 1L7, Canada

Antiinfluenza type 2 (T2) immunity contributes to both immunopathology and immunoprotection, yet the underlying mechanisms modulating T2 immunity remain ill defined. We describe a novel mouse antigen (Ag)-presenting cell (APC), designated late-activator APC (LAPC). After pulmonary influenza A (H1N1) virus infection, LAPCs enter the lungs, capture viral Ag, and subsequently migrate to the draining lymph node (DLN) and spleen, with delayed kinetics relative to dendritic cells (DCs). In the DLN, influenza virus–activated LAPCs present Ag and selectively induce T helper type 2 (Th2) effector cell polarization by cell–cell contact–mediated modulation of GATA-3 expression. In adoptive transfer experiments, influenza virus–activated LAPCs augmented Th2 effector T cell responses in the DLN, increased production of circulating antiinfluenza immunoglobulin, and increased levels of T2 cytokines in bronchoalveolar lavage fluid in recipient influenza virus–infected mice. LAPC-recipient mice exhibited exacerbated pulmonary pathology, with delayed viral clearance and enhanced pulmonary eosinophilia. Collectively, our results identify and highlight the importance of LAPCs as immunomodulators of T2 immunity during influenza A virus infection.

CORRESPONDENCE
Eleanor N. Fish:
en.fish@utoronto.ca

Abbreviations used: Ag, antigen; BAL, bronchoalveolar lavage; cDC, conventional DC; CVB3, coxsackievirus B3; DEAD, direct ex vivo Ag detection; DLN, draining LN; LAPC, late-activator APC; MFI, mean fluorescence intensity; mPDCA-1, mouse pDC Ag 1; pDC, plasmacytoid DC; T1, type 1; T2, type 2; TSLPR, thymic stromal lymphopoietin receptor; VACV, vaccinia virus.

Influenza viruses are common respiratory pathogens associated with considerable morbidity and mortality worldwide (Cox and Subbarao, 2000). Influenza A viruses primarily infect respiratory epithelial cells and replicate to produce large numbers of progeny virus that can then infect alveolar macrophages. Within hours, alveolar macrophages produce proinflammatory cytokines and chemokines, leading to the migration of peripheral blood DCs as well as lymphocytes to the site of infection, and their subsequent activation (La Gruta et al., 2007).

Influenza virus infection induces both type 1 and 2 (T1 and T2, respectively) immune responses (Doherty et al., 2006; La Gruta et al., 2007). T1 immunity, characterized by high levels of IFN-γ and TNF, is predominantly induced by DCs and macrophages, and results in the generation of various effector cells, including Th1 T cells and CTLs, that invoke cell-mediated protective immunity (Doherty et al., 2006; La Gruta et al., 2007). The contributions of T2 immune responses to effective recovery from influenza virus infection are well recognized: Th2 T cell–directed expansion, differentiation, and isotype switching of B cells results in the production of neutralizing antibodies (Clements et al., 1986; Garcon et al., 1990; Marshall et al., 1999). These antibodies have a pivotal role in viral clearance and protection from secondary infection (Palladino et al., 1995; Renegar et al., 2004). Influenza virus–induced T2 immune responses are also linked to immunopathology in primary infection. Pulmonary eosinophilia, a classical T2 inflammatory response associated with influenza virus infection (van der Klooster et al., 2004; Buchweitz et al., 2007), can be induced by T2 proinflammatory cytokines such as IL-5 and eotaxin when expressed in lung tissues and is exacerbated after adoptive transfer of antiinfluenza Th2 T cell clones (Graham et al., 1994; Roboz and Rafii, 1999; Fort et al., 2001; Hurst et al., 2002). Influenza virus infection may also induce nonrespiratory complications, including postinfectious encephalitis (La Gruta

The Rockefeller University Press $30.00
J. Exp. Med. Vol. 207 No. 7 1435-1451
www.jem.org/cgi/doi/10.1084/jem.20091373

et al., 2007). In a mouse model of infection, the levels of T2 cytokines correlated directly with the severity of postinfectious encephalitis induced by primary influenza virus infection (Kaji et al., 2000). Viewed collectively, the data suggest that T2 immunity influences both immunoprotection and immunopathology after influenza virus infection. However, the mechanisms modulating antiinfluenza T2 immune responses remain poorly defined.

In this study, we describe a novel APC population in naive mice, designated late-activator APCs (LAPCs; mouse plasmacytoid DC [pDC] antigen [Ag] 1 [mPDCA-1]$^+$CD11c$^-$TCRβ^-B220$^-$CD38$^+$CD44^{int}CD45$^+$Gr1$^+$). Our morphological, phenotypic, and genetic characterizations of these LAPCs suggest that they are a unique cell population distinct from other immune cell types. In response to pulmonary influenza A virus infection, LAPCs function as APCs in the draining LN (DLN) and spleen. In contrast to DCs, LAPCs exhibit delayed kinetics of migration to the DLN, suggesting a distinct functional role in the DLN. Notably, LAPC trafficking from infected tissues to the associated DLNs was also observed after respiratory infection with vaccinia virus (VACV) and cardiotropic infection with coxsackievirus B3 (CVB3). In ex vivo studies, we provide evidence that influenza virus–activated LAPCs in the DLN induce Th2 effector cell polarization. In vivo adoptive transfer experiments confirmed that influenza virus–activated LAPCs selectively induce both systemic and local antiinfluenza virus T2 immunity in mice. Viewed collectively, the data suggest that these novel APCs may play a pivotal role in modulating antiinfluenza T2 immunity during acute virus infection.

RESULTS

Identification of LAPCs in mice

As previously described (Blasius et al., 2006), the anti–mPDCA-1 mAb recognizes Ag expressed on pDCs (CD11c^{int}B220$^+$CD11b$^{low/-}$CD8$\alpha^{low/-}$CD4$^+$Gr1$^+$) and some B(B220$^+$CD19$^+$)andCD4$^+$T(CD4$^+$CD8α^-CD49b$^-$TCRβ^+) lymphocytes (Fig. 1 A and not depicted). Interestingly, in LNs from naive C57BL/6J mice, we identified another mPDCA-1 Ag–positive cell population, defined in this study as LAPCs, that is CD11c$^-$, TCRβ^-, and B220$^-$ (Fig. 1 B). Further phenotypic characterization of these LAPCs revealed that this cell population is CD38$^+$, CD44^{int}, CD45$^+$, and Gr1$^+$ (Fig. 1 C). LAPCs (mPDCA-1$^+$CD11c$^-$TCRβ^-B220$^-$CD38$^+$CD44^{int} CD45$^+$Gr1$^+$) were also detected in the spleens of naive mice and exhibited an identical pattern of cell-surface marker expression to LN-derived LAPCs (unpublished data).

Because CD38 and CD44 are markers for B and T lymphocytes, respectively (Oliver et al., 1997; Maiti et al., 1998), we examined whether LAPCs represent a developmental stage of lymphocytes by using splenocytes from Rag-1 knockout mice (Rag-1$^{-/-}$) and their WT littermates (Rag-1$^{+/+}$; Fig. 1 D). Despite major defects in lymphocyte development (unpublished data), in replicate experiments we identified LAPCs in Rag-1$^{-/-}$ mice with <100,000 cells detected per spleen. Moreover, statistical analysis revealed no significant difference in LAPC numbers between Rag-1$^{-/-}$ and Rag-1$^{+/+}$ mice ($P = 0.198$), from which we infer that these cells are not mature lymphocytes.

To determine whether LAPCs originate from either DCs or NK cells, the number of splenic LAPCs was compared between Flt3L$^{-/-}$ or IL-15$^{-/-}$ mice and their WT littermates. Flt3L$^{-/-}$ mice exhibit a selective defect in both DC and NK cell development, and IL-15$^{-/-}$ mice exhibit a selective defect in NK cell development (unpublished data; Kennedy et al., 2000; McKenna et al., 2000). However, we identified no significant decrease in LAPC numbers in the spleens of these Flt3L$^{-/-}$ and IL-15$^{-/-}$ mice compared with WT littermates (Fig. 1 D). Rather, in these mice, we detected an increase in LAPC numbers in spleens. As for Id2$^{-/-}$ mice, for which Id2 is a critical determining factor for NK cell and DC development, thereby leading to a selective defect in the development of Langerhans cells and CD8α^+ DCs, but skewing the phenotype toward increased numbers of mature B cells in the periphery (Becker-Herman et al., 2002; Hacker et al., 2003), this increase in splenic LAPC numbers may be a consequence of skewing of lineage-determinant factors. Our results suggest that LAPCs follow a different developmental pathway to that of either DCs or NK cells.

To further delineate the relationship of LAPCs to other immune cell types, gene expression analysis was performed comparing the expressed signature gene profile of LAPCs with other immune cell types. LAPCs were isolated from the mediastinal DLNs of either mock (PBS) or A/WSN/33 influenza virus–infected mice (500 PFU, intranasal) on day 8 after infection. Cells were lysed, RNA extracted, and processed for analysis by the Affymetrix GeneChip platform. Using public databases, we compared the gene expression profiles of LAPCs with other mouse immune cell types, including B cells, CD4$^+$ T cells, CD8$^+$ T cells, NK cells, CD11b$^+$ conventional DCs (cDCs), CD8α^+ cDCs, pDCs, macrophages, granulocytes, and mast cells. Unsupervised hierarchical clustering analysis of 36,290 probe sets across 11 different cell types was performed using GeneSpring analysis software (version 10). This global gene expression profile comparison revealed several biological trends (Fig. 2). Overall, the phylogenetic tree replicated previous results by Robbins et al. (2008) in relation to the cell-type comparisons performed in this study. Three main subbranches occur, which fall across three biological classifications: lymphocytes, DCs, and myeloid cells. According to this clustering scheme, LAPCs fall into the myeloid lineage and are most similar in gene expression profile to granulocytes.

We next undertook to compare the signature gene expression profiles between LAPCs and each individual immune cell type. Notably, these direct comparisons between LAPCs and 10 other immune cell types revealed a distinguishable gene expression signature for LAPCs, distinct even from granulocytes (Table S1). Of note, because LAPCs show no CD3ε or pre-TCRα gene expression, this is in further support that LAPCs differ in their origin from lymphocytes and DCs (Corcoran et al., 2003).

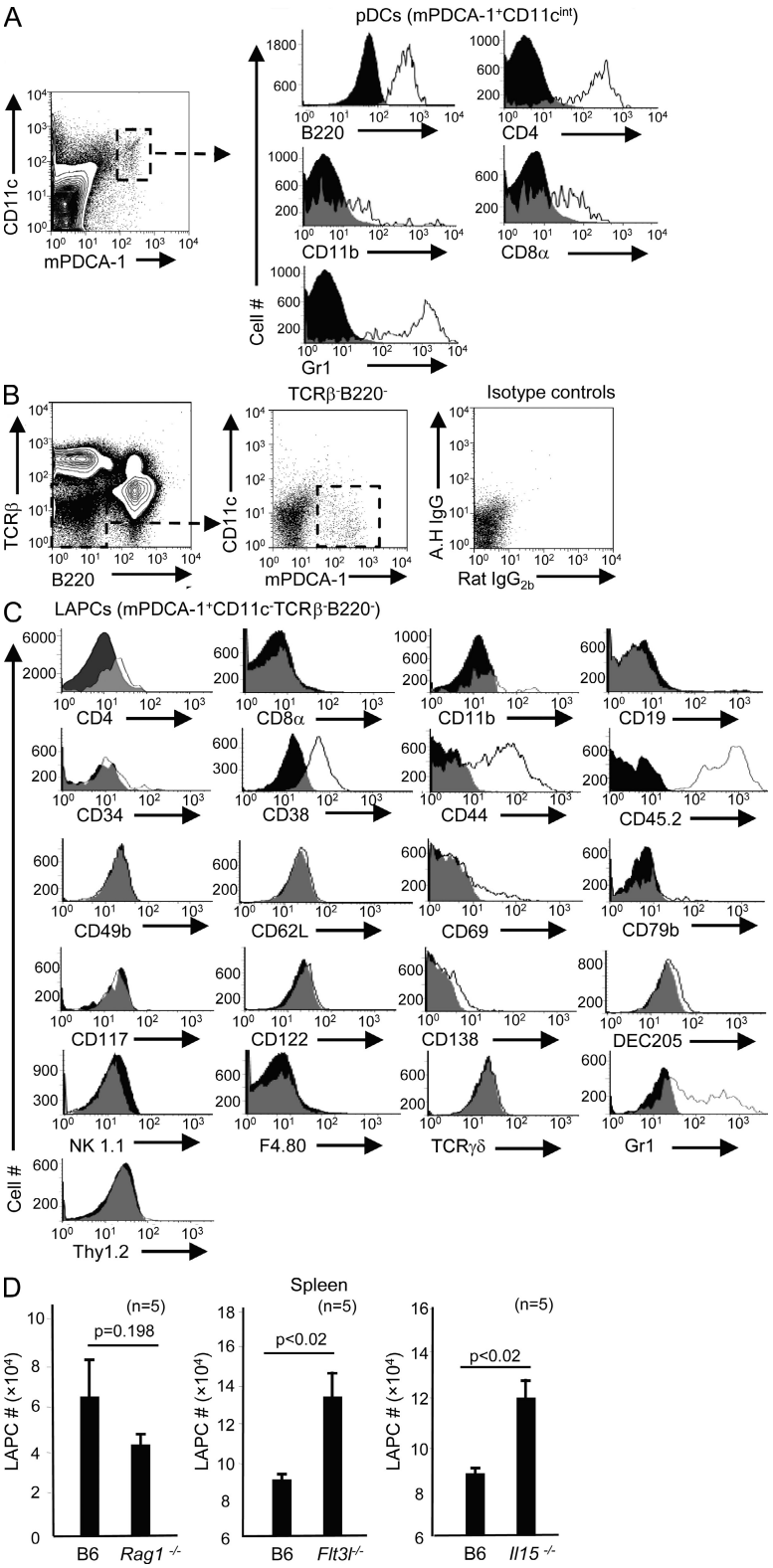

Figure 1. Phenotypic characterization of LAPCs. Inguinal and axillary LNs were harvested from naive C57BL/6J mice aged 8–12 wk, and single-cell suspensions were prepared and processed for flow cytometry as described in Materials and methods. (A) Lineage-specific markers were examined on pDCs (open histograms). Staining with isotype-matched control antibodies was included (black histograms; $n = 3$ mice). (B) TCRβ$^-$B220$^-$ cells were characterized using mPDCA-1– and CD11c-specific mAbs. Isotype control staining is also shown ($n = 3$ mice). (C) LAPCs (mPDCA-1$^+$CD11c$^-$TCRβ$^-$B220$^-$) were stained with antibodies specific for the indicated surface markers (open histograms). Staining with isotype-matched control antibodies was included (black histograms; $n = 3$ mice). For A–C, representative staining from at least five independent experiments ($n = 3$ for each experiment) is shown. (D) Splenocytes were isolated from the indicated gene-targeted mice and WT C57BL/6J mice ($n = 5$ each), and stained for markers of LAPCs (mPDCA-1$^+$ CD11c$^-$TCRβ$^-$B220$^-$). LAPCs are recorded as absolute cell numbers (means ± SEM) in total splenocytes based on their percentage in the total cell population. Data are representative of two independent experiments and were analyzed using a Student's *t* test. A.H IgG, Armenian hamster IgG.

Although LAPCs express the neutrophil marker Gr1 (Fleming et al., 1993) and are most similar to granulocytes in their global gene expression profile, their morphology does not conform with that of granulocytes. In agreement with our purity data (>97% with <1% contamination with CD11c$^+$; unpublished data), LAPCs present as a homogeneous cell population with morphological characteristics of plasmacytoid cells, namely a round shape, distinct from DCs (pDCs, mPDCA-1$^+$CD11c^{int}; cDCs, CD11c^{high} B220$^-$) and B (B220$^+$CD19$^+$) and T (TCRβ$^+$) lymphocytes (Fig. 3, A and B). LAPCs have a smooth plasma membrane with no pseudopodia. The cytoplasm has no granules, fewer organelles (vacuoles and mitochondria), and a denser appearance than DCs. There is also a marked difference in the shape of the nuclei between LAPCs and DCs, with LAPC nuclei being uniformly large and round. Viewed collectively, these data distinguish LAPCs from PMNs, granulocytes, DCs, macrophages, lymphocytes, and NK cells.

In an attempt to identify LAPC-specific genes, another round of gene expression analysis was performed. 279 genes were identified that displayed a 10-fold difference in expression level between LAPCs and any other immune cell lineage in at least 5 out of the 10 possible comparisons (unpublished data). Further analysis provided a list of 20 gene candidates apparently not expressed by other immune cell types (Affymetrix intensity value < 100) except LAPCs (Affymetrix intensity value > 100; Fig. S2). Interestingly, this list includes some reproduction-related genes such as *Oosp1*, *Plac1l*, and *Pp11r*. In addition, several membrane-bound ion channel–related genes were identified, including *Cacna1h* and *Atp6v0a1*. *Reln* (extracellular matrix serine protease), which is

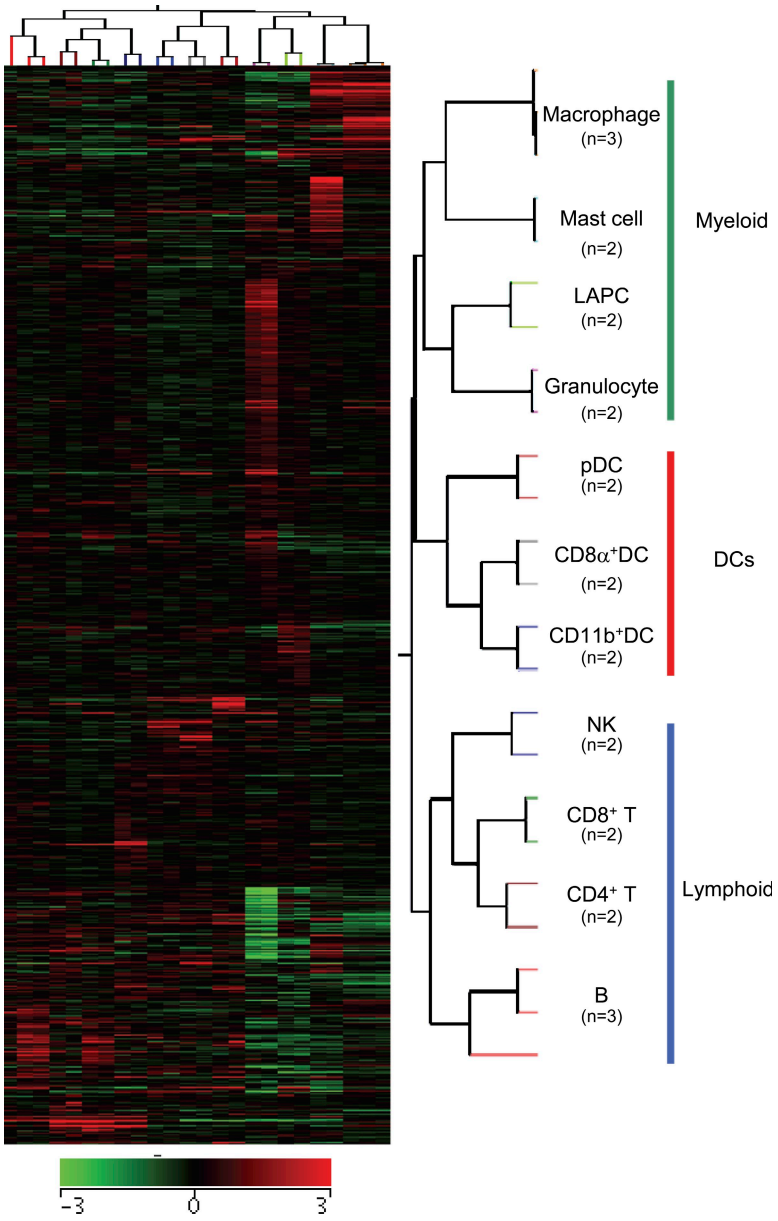

Figure 2. LAPCs exhibit a unique gene expression signature. Two-way unsupervised hierarchical clustering analysis using microarray gene expression data for multiple immune cell types, including LAPCs. Data are visualized colorimetrically with heat plots (red represents elevated gene expression and green represents decreased gene expression). The color scale for relative expression values as obtained after $\log_2$ transformation and median centering of the values across samples for each gene is given below the heat map. The experimental analysis was performed as described in Materials and methods.

one of the key neuronal proteins regulating brain development, is also highly expressed by LAPCs regardless of their activation status. Moreover, *Tnfrsf17/Bcma*, most commonly associated with plasma cells, was identified, even though our gene expression data and results from the Rag-$1^{-/-}$ mice studies suggest that LAPCs are not mature B lymphocytes. In preliminary studies examining expression of BCMA and Plac1l by FACS, we confirmed that LAPCs express both, albeit at low levels (unpublished data). The combination of these cell surface–expressed factors and mPDCA-1, CD38, CD44, CD45, and Gr1 in the absence of CD11c, TCRβ, B220, and CD19 further support the evidence that LAPCs are distinct from other immune cell types.

Further screening for this rare cell population revealed that LAPCs populate peripheral blood and lymphoid tissues including BM, LNs, and spleens in naive C57BL/6J mice (Table I). Notably, in spleens, the cell numbers are comparable to pDCs. LAPCs were identified in all mouse strains we have screened, including BALB/c, A/J, and DBA/2J mice (Fig. S3).

LAPCs are APCs responding to virus infection

LAPCs derived from LNs express both MHC-II (I-A/E) and co-stimulatory molecules such as CD40, CD80, and CD86, although expression levels are lower than identified for DCs (Fig. 4 A). Splenic LAPCs exhibit a similar pattern of cell-surface Ag expression, albeit MHC-II, CD40, and CD80 levels are modestly higher (mean fluorescence intensity [MFI] = 467 ± 145, 63 ± 19, and 83 ± 25, respectively; unpublished data) compared with their expression levels on LAPCs derived from LNs (MFI = 177 ± 9, 14 ± 1, and 28 ± 4, respectively).

To examine the effects of virus infection on the activation and migration of LAPCs, mice were intranasally instilled with a sublethal dose (500 PFU) of influenza virus (A/WSN/33). In time-course studies, we observed that LAPCs in the DLN (mediastinal LN) up-regulated surface expression of MHC-II, CD40, and CD86 molecules in a similar manner to both pDCs and cDCs (Fig. 4 B). However, the expression levels of these co-stimulatory molecules on LAPCs were lower than identified for DCs on day 3 after infection. Notably, LAPCs were detected in the secondary lymphoid tissues (LNs and spleen) of both naive and A/WSN/33 influenza virus–infected mice (day3), together with cDCs and pDCs, as a distinct population in the contour plots of CD11c and MHC-II coexpression, in further support that LAPCs are a unique population distinct from DCs (Fig. 4 C).

In response to pulmonary influenza A virus infection, the population of LAPCs increased in the lungs early after infection (approximately day 3 after infection) and declined thereafter. A significant increase in LAPCs in the DLN and spleen, but not in the nondraining LNs (inguinal and axillary LNs), was observed later after infection, on day 6 (Fig. 4, D and E). Notably, the greatest number of LAPCs in the DLN and spleen was observed on day 8 after infection, whereas, as previously

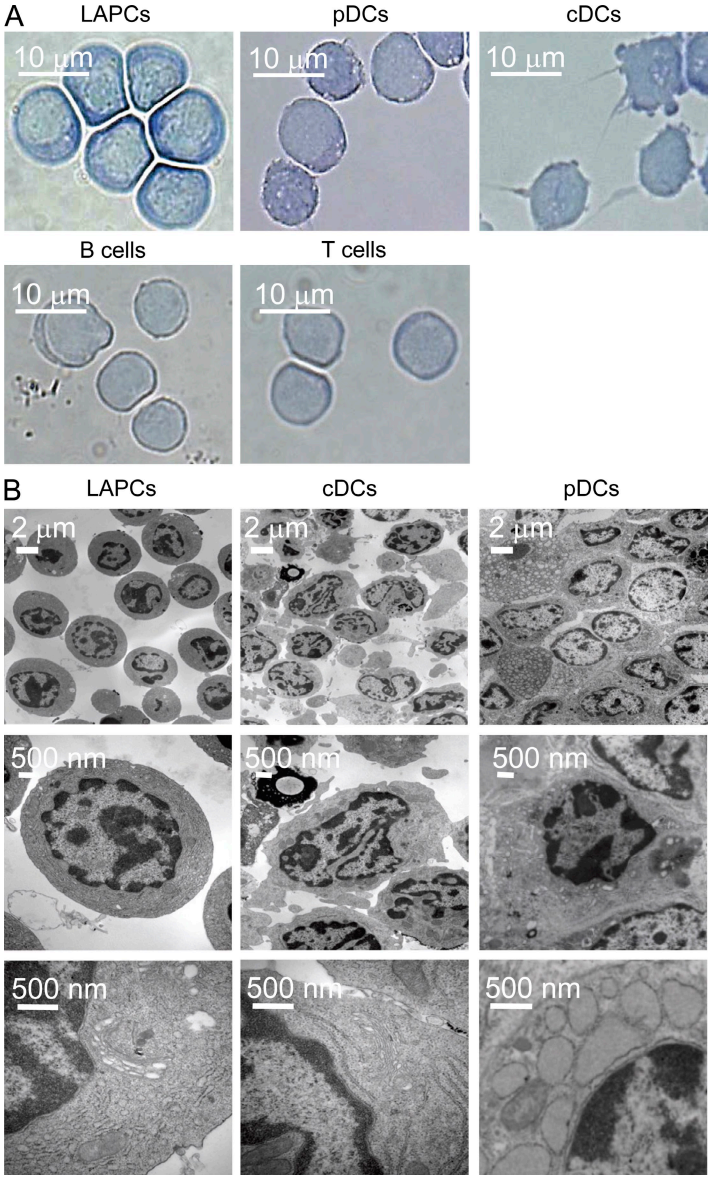

Figure 3. Morphological characterization of LAPCs in naive mice. (A) Representative images of the indicated cell types: LAPCs (mPDCA-1$^+$CD11c$^-$TCRβ$^-$B220$^-$), pDCs (mPDCA-1$^+$CD11c^{int}), cDCs (CD11c^{high}B220$^-$), B cells (B220$^+$CD19$^+$), and T cells (TCRβ$^+$). Each cell population was FACS sorted from either LNs or spleens isolated from naive C57BL/6J mice, cytocentrifuged, and stained with modified Wright-Giemsa. (B) Representative ultrastructure details of freshly isolated LAPCs, cDCs, and pDCs using transmission electron microscopy. Representative images from two independent experiments are shown.

reported (Yoneyama et al., 2005), DCs were most abundant in the DLN on day 3 after infection.

Although we cannot rule out the possibility that influenza virus–activated LAPCs may proliferate in the lungs or DLN, our data from in vivo Ag uptake (FITC-dextran; Fig. 5, A and B) and migration (CFSE; Fig. 5, C and D) experiments suggest that lung-infiltrated LAPCs capture viral Ags and migrate to the DLN and spleen in response to influenza virus infection, presumably to stimulate cognate CD4$^+$ T cells. In Rag-1$^{-/-}$, Flt3L$^{-/-}$, and IL-15$^{-/-}$ mice infected intranasally with 250 PFU of influenza A virus, we could still observe significant LAPC infiltration into the spleen, further corroborating that these cells are neither lymphocytes, DCs, nor NK cells (unpublished data). LAPC migration to the lungs, DLN, and spleen was a specific response to inflammation induced by influenza A virus infection, because no infiltrates were seen in mock-infected (FITC-dextran, CFSE, IMDM, and PBS) mice (Fig. 5, B and D; and not depicted). In addition, we did not observe any sex differences in the activation of LAPCs by influenza virus infection, because both male and female mice showed similar levels of cell infiltration into the DLN (unpublished data). Influenza virus–activated LAPCs on day 8 after infection showed identical surface marker expression to that of naive LAPCs (unpublished data) and did not exhibit morphological changes beyond enlargement (unpublished data).

Given that chemokines regulate leukocyte recruitment to the lung during the early phase of influenza infection, and the evidence that CXCR3–CXCL10 interactions influence this trafficking (Dawson et al., 2000; Wareing et al., 2004; La Gruta et al., 2007), we examined bronchoalveolar lavage (BAL) fluid for CXCL10 production and LAPCs for CXCR3 expression. CXCL10 was detectable in the lungs from day 3 after infection, with maximal production on day 6 (Fig. S4 A). In naive mice, circulating LAPCs express CXCR3 on their surface. Early (day 3) in influenza virus infection, LAPCs infiltrating the lung continue to express CXCR3. However, CXCR3 expression was significantly down-regulated by day 6 after infection in lung-derived LAPCs and could not be detected on LAPCs in the DLN (Fig. S4 B). These results suggest that the early inflammation in influenza virus–infected lung tissue might induce the infiltration of circulating LAPCs into the lungs, presumably mediated by CXCR3–CXCL10–induced chemotaxis. Subsequently, influenza virus–activated LAPCs down-regulate CXCR3 expression and thereafter migrate to the DLN.

To determine the potential of LAPCs to function as APCs in the DLN, we performed a direct ex vivo Ag detection (DEAD) assay. C57BL/6J mice were instilled intranasally (500 PFU) with either WT influenza A virus (A/WSN/33) or recombinant virus expressing MHC-II–restricted OVA peptide (323–339; A/WSN/OVA(II)). On day 3 after infection, one group of mice was sacrificed and DCs (cDCs and pDCs) were harvested from the DLN, and on day 8 after infection, the remaining mice were sacrificed and LAPCs were harvested from the DLN. Naive OT-II T cells were cultured with either day 3 DCs or day 8 LAPCs, which were then either restimulated at 96 h with PMA and ionomycin, or not.

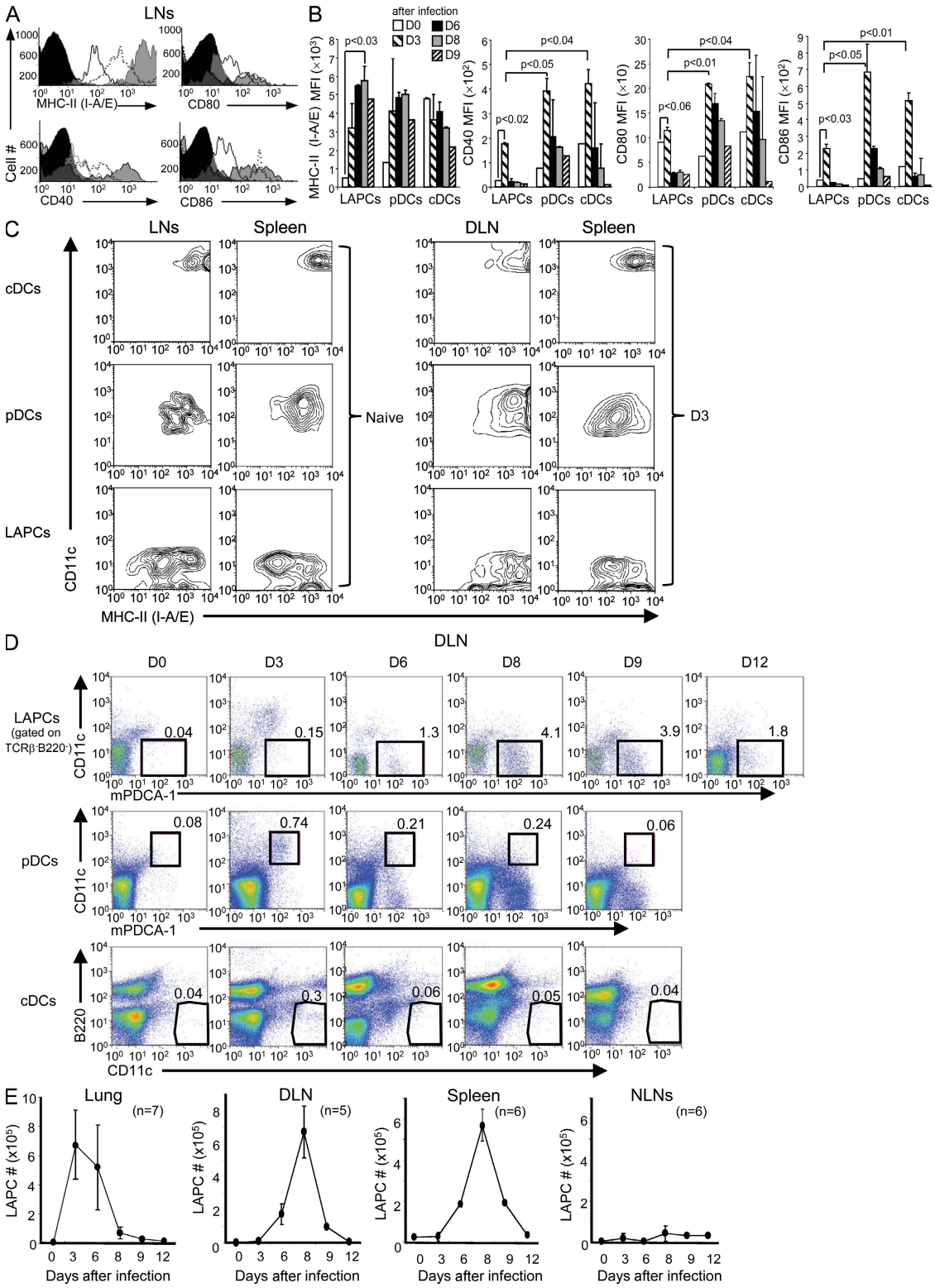

Figure 4. LAPCs exhibit characteristics of APCs responding to pulmonary influenza virus infection. (A) LN single-cell suspensions from naive C57BL/6J mice (n = 3) were stained with antibodies specific for MHC-II (I-A/E), CD40, CD80, and CD86. Histograms are gated on LAPCs (mPDCA-1$^+$ CD11c$^-$TCRβ$^-$B220$^-$; continuous line open histograms), pDCs (mPDCA-1$^+$CD11c^{int}; dashed line open histograms), and cDCs (CD11c^{high}B220$^-$; gray histograms). Staining with isotype-matched control antibodies was included (black histograms). Data are representative of three independent experiments. (B) C57BL/6J mice (n = 15) were infected intranasally with 500 PFU of A/WSN/33 influenza virus. At the indicated times after infection, mice were sacrificed and DLNs were harvested. Cells were collected and stained with the appropriate fluorochrome-conjugated mAbs to monitor surface expression of

Table I. Percent population of LAPCs in different lymphoid tissues of naive C57BL/6J mice

	LAPCs (mPDCA-1$^+$CD11c$^-$TCRβ$^-$B220$^-$)	pDCs (mPDCA-1$^+$CD11c^{int})	cDCs (CD11c^{high}B220$^-$)
LNs (n = 12)	0.045 ± 0.006	0.075 ± 0.006	0.14 ± 0.02
Spleen (n = 12)	0.12 ± 0.01	0.11 ± 0.02	0.92 ± 0.1
PBMCs (n = 10)	0.13 ± 0.03	0.06 ± 0.02	0.06 ± 0.03
BM (n = 10)	0.45 ± 0.2		
Thymus (n = 10)	0.02 ± 0.01		

Data shown are means ± SD.

LAPCs from A/WSN/OVA(II) virus–infected mice activated OT-II T cells to produce IL-2 (Fig. 5 E). T cell activation was further confirmed by a [^{3}H]thymidine incorporation assay, which demonstrated that influenza virus–activated LAPCs isolated from the DLN on day 8 after infection exhibited equivalent activity to DCs harvested on day 3 after infection (Fig. S5).

To examine whether Ag presentation by LAPCs still occurs in mice with defects in DC development, another series of DEAD assays was performed using LAPCs isolated from the DLNs of influenza virus–infected (250 PFU) Flt3L$^{-/-}$ mice. As shown in Fig. S6, LAPCs isolated from Flt3L$^{-/-}$ mice on day 8 after infection presented viral Ag to cognate CD4$^+$ T cells. Moreover, LAPCs from Flt3L$^{-/-}$ mice (250 PFU) exhibited even higher Ag-presenting capacity than that of LAPCs from WT mice (500 PFU; Fig. 5 E), suggesting that LAPCs are indeed a unique APC population distinct from DCs.

Next, we examined whether LAPCs respond to other virus infections. CVB3 induces myocarditis and dilated cardiomyopathy in mice (Baboonian et al., 1997). C57BL/6J mice were infected with 10,000 PFU CVB3 by intraperitoneal injection and then monitored on days 3 and 7 after infection for LAPC migration into the DLN (mediastinal LN). As with influenza virus infection, maximal infiltration of LAPCs was observed at the later time point, day 7 after infection (unpublished data). As the vaccine agent for smallpox, VACV is one of the most well-characterized members of the poxvirus family (Smith and Law, 2004). Using the recombinant strain Western Reserve VACV (10,000 PFU) to infect C57BL/6J mice by intranasal inoculation, we again observed LAPC migration to the DLN, with the greatest number detected by day 7 after infection (unpublished data). Viewed collectively, these data suggest that LAPCs are APCs distinct from DCs, responding to various virus infections including influenza virus, CVB3, and VACV.

Influenza virus–activated LAPCs localize in T cell zones of the DLN

To examine the localization of Ag-presenting influenza virus–activated LAPCs in the DLN, an in vivo tracking experiment was performed using CFSE labeling. Influenza A virus–activated LAPCs isolated on day 6 after infection from the DLNs of mice were stained with CFSE in vitro and adoptively transferred by i.v. injection into influenza virus–infected recipient mice on day 6 after infection. 24 h after transfer, the DLNs were harvested from recipient mice and the localization of donor LAPCs was monitored by confocal microscopy (Fig. 6 A). As shown in Fig. 6 B, the majority of CFSE-labeled donor LAPCs localized to the T cell zone (B220$^-$ area) and some localized to the paracortex region (boundary of the B and T cell zones) of the DLN. However, few donor LAPCs localized to the B cell zone (B220$^+$ area).

Influenza virus–activated LAPCs induce Th2 polarization of Ag-primed CD4$^+$ T cells ex vivo

Given the localization of Ag-presenting LAPCs to the T cell zone in the DLN, we examined whether influenza virus–activated LAPCs are capable of modulating antiinfluenza CD4$^+$ T cell responses in the DLN. To do this, we designed a system to mimic T cell–LAPC interactions in the DLNs. Specifically, OT-II T cells were purified from naive Thy1.1$^+$ OT-II mice and transferred into Thy1.2$^+$ C57BL/6J mice (2–3 × 10^6 cells/mouse) by i.v. injection.

24 h after adoptive transfer, recipient mice were infected by intranasal instillation with 500 PFU of A/WSN/OVA(II) virus. On day 5 after infection, after the accelerated migration of DCs from lung to the DLN and before the significant influx of LAPCs (Fig. 4 D), in vivo Ag-primed OT-II T cells (Thy1.1$^+$CD4$^+$) were isolated from the DLN and cultured together with either DCs or LAPCs sorted from the DLNs of either A/WSN/33 or A/WSN/OVA(II) influenza virus–infected mice harvested on day 8 after infection. 24 h after

the indicated molecules for each cell population. Data are representative of two independent experiments and presented as MFI (means ± SD). (C) Single-cell suspensions were isolated from each indicated lymphoid tissue from naive or A/WSN/33 influenza virus–infected C57BL/6J mice (D3) and stained with the appropriate fluorochrome-conjugated mAbs. The coexpression of MHC-II (I-A/E) and CD11c for each gated population (cDCs, pDCs, and LAPCs) is shown as contour plots. Data are representative of three independent experiments. (D) At the indicated times after infection, the abundance of LAPCs, pDCs, and cDCs in the DLN was monitored, presented as the percent population in total DLN cells (n = 5 mice at each time point). Representative staining from three independent experiments is shown. (E) At the indicated times after infection, the absolute numbers of LAPCs in the lungs (n = 7 at each time point), DLN (n = 5 at each time point), spleens (n = 6 at each time point), and nondraining inguinal and axillary LNs (NLNs; n = 6 at each time point) was monitored. Data are representative of three independent experiments and are shown as means ± SD.

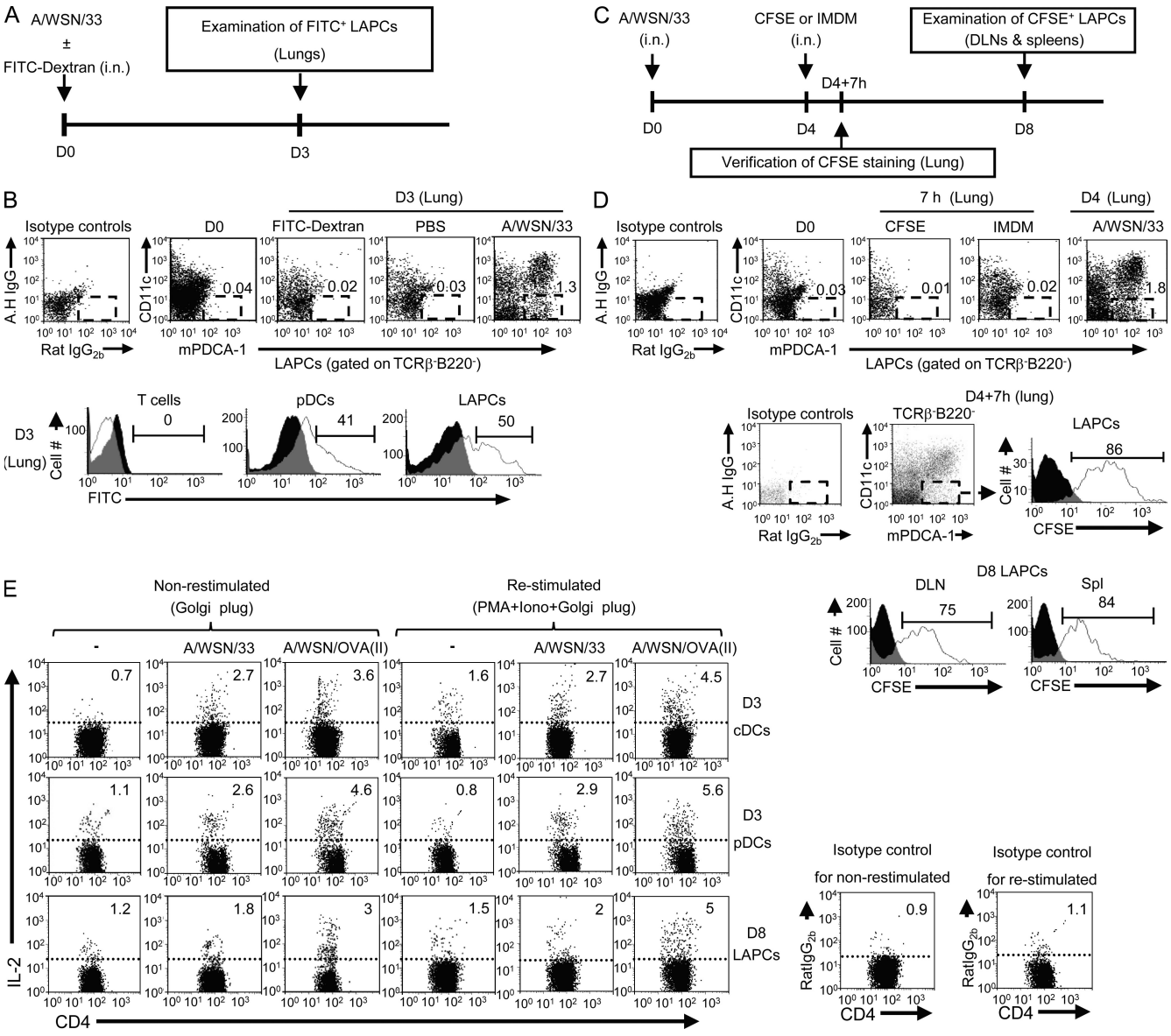

Figure 5. Influenza virus–activated LAPCs transport viral Ags from the lungs to the DLN and spleen for Ag presentation. (A) Schematic diagram for in vivo Ag uptake assay. (B) Mice (n = 12) were infected intranasally with 500 PFU of A/WSN/33 virus with or without (negative control) FITC-dextran. On day 3 after infection, mice were sacrificed and FITC+ T cells, pDCs, and LAPCs were examined in the lungs from FITC-dextran–instilled (open histograms) or control (black histograms) mice by FACS analysis. Numbers indicate the percentage of FITC+ cells within each population. As additional controls, naive mice were instilled only with FITC-dextran or sterile PBS and sacrificed on day 3 after treatment. Dot plots are gated on the TCRβ−B220− cell population in the lungs; the presence of LAPCs (mPDCA-1+CD11c−) was monitored and compared with lung LAPCs derived from day 0 and 3 influenza virus–infected mice. Numbers indicate the percent population in total lung cells. Data are representative of two independent experiments. (C) Schematic diagram for in vivo migration assay. (D) Mice (n = 12) were infected with 500 PFU of A/WSN/33 virus. On day 4 after infection, mice received an intranasal instillation with either CFSE or carrier medium (sterile IMDM; negative control). At the indicated time points after infection, mice were sacrificed (n = 3 for each time point) and the CFSE+ LAPC population in the indicated tissues of CFSE-instilled (open histograms) or sterile IMDM-instilled (black histograms) mice was examined by FACS analysis. Numbers indicate the percentage of CFSE+ LAPCs. As additional controls, naive mice were instilled only with CFSE or sterile IMDM and sacrificed at 7 h after treatment. The presence of LAPCs was monitored and compared with lung LAPCs derived from day 0 and 4 influenza virus–infected mice. Numbers in dot plots show the percent population in total lung cells. Data are representative of two independent experiments. (E) Mice were infected with 500 PFU of A/WSN/33 (n = 15) or A/WSN/OVA(II) (n = 15) virus. On day 3 after infection, mice were sacrificed and DCs (cDCs and pDCs; n = 10 mice) were isolated from the DLN. On day 8 after infection, LAPCs (n = 5 mice) were isolated from the DLN. Naive OT-II T cells were cultured with day 3 DCs or day 8 LAPCs. IL-2 production from OT-II cells was examined on day 4 after incubation by intracellular cytokine staining. The horizontal dotted lines indicate the gate above which the IL-2–positive cell population is defined relative to the rat IgG_{2b} isotype control. Representative staining from at least three independent experiments is shown. A.H IgG, Armenian hamster IgG.

incubation, the generation of effector $CD4^+$ T cells was examined by intracellular FACS staining for both IFN-γ and IL-4.

When isolated on day 5 after infection, >91% of the in vivo Ag-primed OT-II T cells exhibited an activated phenotype, expressing elevated levels of CD44 and CD69 and decreased levels of CD62L compared with naive OT-II T cells. Approximately 80% of these in vivo primed OT-II T cells exhibited an effector ($CD44^{high}CD62L^{low}$) or memory ($CD44^{high}CD62L^{high}$) phenotype (Fig. 7 A), and ∼6% had differentiated into IFN-γ–producing Th1 effector cells (Fig. 7 B), presumably mediated by the cognate interaction with influenza virus–activated DCs in the DLN at an early phase of influenza A virus infection (Cella et al., 2000; GeurtsvanKessel et al., 2008). When co-cultured for 24 h with either DCs ($CD11c^+TCR\beta^-$) or LAPCs ($mPDCA\text{-}1^+CD11c^-TCR\beta^-B220^-$) derived from A/WSN/33 or A/WSN/OVA(II) virus–infected mice, a proportion of in vivo Ag-primed OT-II T cells differentiated into Th2 effector cells producing both IL-4 and IL-10 (Fig. 7 C). For optimal Th2 polarization, the cognate interaction with Ag-presenting LAPCs derived from A/WSN/OVA(II) virus–infected mice was required. However, there was no additive effect on Th2 polarization by incubation with DCs derived from A/WSN/OVA(II) virus–infected mice compared with DCs from A/WSN/33 virus–infected mice. Moreover, OT-II T cells incubated with LAPCs from A/WSN/OVA(II) virus–infected mice showed a higher capacity for Th2 polarization compared with OT-II T cells incubated with DCs from the same mice. Collectively, the data suggest that DCs in the DLN on day 8 after infection may not present viral Ag to $CD4^+$ T cells but that LAPCs may function as APCs by modulating antiinfluenza Th2 effector T cell responses in the DLN at this later time point after infection.

This result was further confirmed using only activated OT-II T cells. On day 5 after infection, OT-II T cells exhibiting an activated phenotype ($CD44^{high}CD62L^{high}$, $CD44^{high}CD62L^{low}$, and $CD44^{int}CD62L^{low}$) were sorted from the DLNs and incubated together with γ-irradiated LAPCs from A/WSN/OVA(II) virus–infected mice (Fig. S7 A). Th2 polarization of Ag-primed OT-II T cells was examined by FACS analysis. As anticipated, ∼4% of Ag-primed OT-II T cells differentiated into a Th2 effector phenotype upon incubation with influenza virus–activated LAPCs presenting cognate Ag (Fig. S7 B).

Soluble factors, possibly produced by influenza virus–activated LAPCs, may be dispensable for LAPC-mediated Th2 polarization, because LAPCs modulated Th2 polarization despite γ irradiation (2,000 rads; Fig. 7 C). This was further supported by Transwell experiments providing evidence that cell–cell contact is necessary for LAPC-mediated Th2 polarization (Fig. 7 E). Furthermore, influenza virus–activated LAPCs selectively induced GATA-3 expression, the master regulator controlling Th2 differentiation (Zheng and Flavell, 1997), from Ag-primed OT-II T cells (Fig. 7 D). Notably, T-bet expression in OT-II T cells was not modulated by incubation with LAPCs. The ability of LAPCs to promote Th2 polarization is

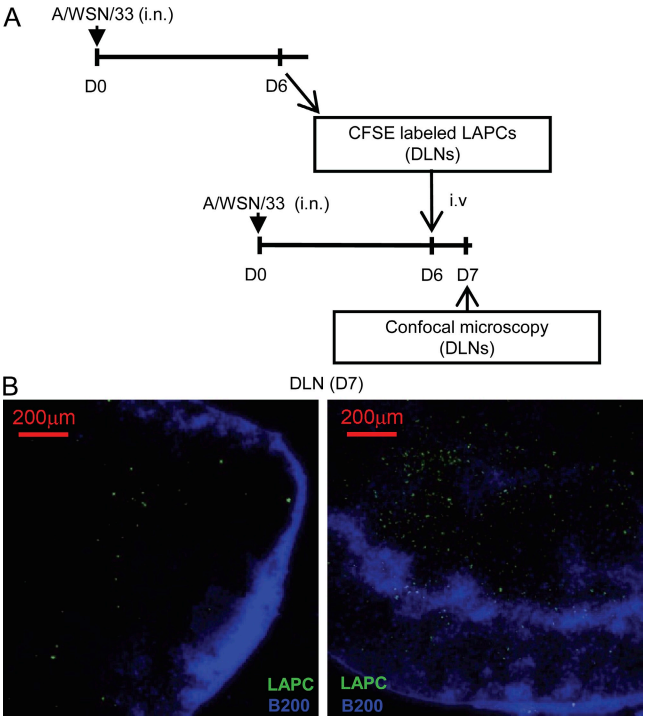

Figure 6. Influenza virus–activated LAPCs localize to the T cell area in the DLN. (A) Mice ($n = 10$) were infected intranasally with 500 PFU of A/WSN/33 virus, and on day 6 after infection, LAPCs were isolated from the DLNs. These LAPCs were CFSE labeled and adoptively transferred (10^6 cells/mouse) into recipient A/WSN/33 virus–infected (500 PFU) mice (day 6 after infection; $n = 2$). (B) 24 h after adoptive transfer, mice were euthanized and the DLNs were harvested and processed as described in Materials and methods for confocal microscopy. Representative images of two independent experiments are shown.

further supported by our observation that maximal Th2 polarization in vivo coincided temporally (day 8) with maximal LAPC infiltration into the DLN after influenza A virus infection (unpublished data). Moreover, LAPCs may express the thymic stromal lymphopoietin receptor (TSLPR), which is implicated in regulating the induction of T2 immunity in both the human and mouse systems (Ziegler and Liu, 2006), at a comparable level to that observed in DCs in naive mice. Notably, *Tslpr* gene expression was down-regulated in LAPCs on day 8 after influenza virus infection (Table S1). The contribution of TSLP–TSLPR–mediated events to LAPC-induced Th2 polarization in our influenza A virus infection model remains to be clarified. Collectively, these results suggest that influenza virus–activated LAPCs induce Th2 effector cell polarization of Ag-primed $CD4^+$ T cells through cell–cell contact–mediated selective modulation of GATA-3 expression coordinated with TCR signaling.

Influenza virus–activated LAPCs modulate antiinfluenza T2 immunity in vivo

The role of LAPCs in modulating antiinfluenza virus T2 immunity was further examined by in vivo adoptive transfer experiments. Either influenza A virus–activated LAPCs or

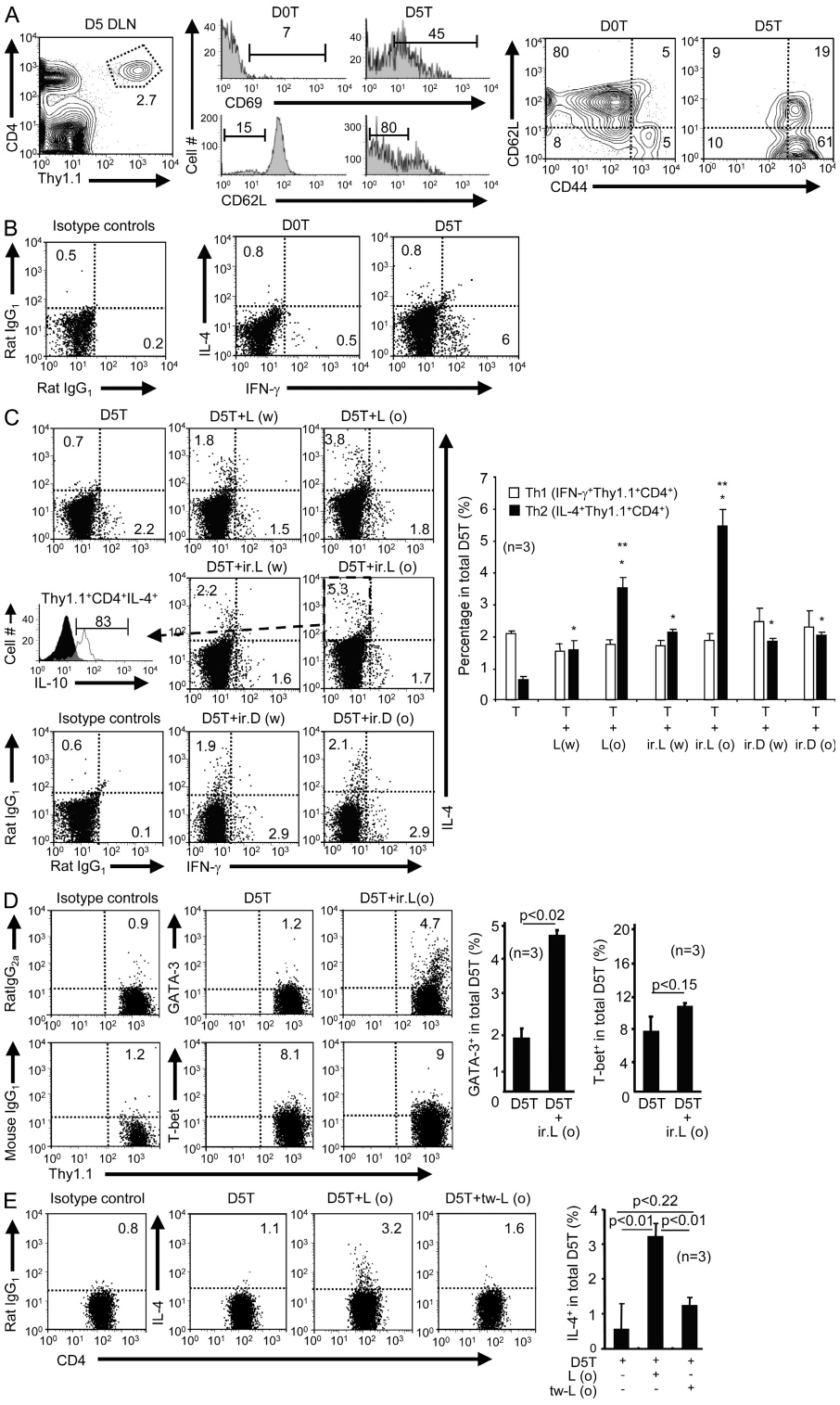

Figure 7. Influenza virus–activated LAPCs induce Th2 effector cell polarization ex vivo. CD4+ T cells were isolated from naive Thy1.1+ OT-II mice and transferred into C57BL/6J (Thy1.2+) recipient mice (2–3 × 10^6 cells/mouse) by i.v. injection. 24 h after adoptive transfer, recipient mice were infected intranasally with 500 PFU of A/WSN/OVA(II) virus. On day 5 after infection, recipient mice (n = 20) were sacrificed and donor T cells (Thy1.1+CD4+) were sorted from the DLN. (A) The activation markers expressed on sorted donor OT-II T cells (D5T, day 5) were compared with those on naive OT-II T cells (D0T, day 0) by flow cytometry. Representative images of three independent experiments are shown. (B) IL-4 and IFN-γ expression in D0T and D5T was examined by intracellular cytokine staining. Representative images of three independent experiments are shown. (C and D) D5T (10^5 cells/well) were cultured with live or γ-irradiated (ir.) LAPCs (L; 5 × 10^4 cells/well) isolated from the DLN of A/WSN/33 (w) or A/WSN/OVA(II) virus (o)–infected C57BL/6J mice on day 8 after infection. γ-Irradiated DCs (CD11c+TCRβ−; ir.D) isolated from the same DLNs were used as controls. At 24 h after incubation, IL-4, IL-10, and IFN-γ production (C) and GATA-3 and T-bet expression (D) were examined in the D5T (Thy1.1+CD4+) population. Representative images of at least three independent experiments are shown. (E) D5T were incubated alone or together with day 8 LAPCs derived from A/WSN/OVA(II) virus–infected mice (L (o)) with or without a Transwell (tw) for 24h. D5T IL-4 expression was measured by intracellular cytokine staining. The horizontal dotted lines indicate the gate above which the IL-4–positive cell population is defined relative to the rat IgG1 isotype control. Data representative of three independent experiments are shown as means ± SEM and were analyzed using a Student's t test. *, $P < 0.05$ compared with D5T only; **, $P < 0.05$ compared with D5T incubated with either L (w) or ir.L (w).

DCs were isolated from the DLNs and spleens of mice on day 8 after infection (300 PFU), and transferred into recipient influenza A virus–infected mice (300 PFU) by i.v. injection on days 1 (3×10^5cells/mouse) and 3 (5×10^5cells/mouse) after infection (Fig. 8 A). A control group of recipient mice received only sterile PBS by i.v. injection, also on days 1 and 3.

Weight loss was monitored on a daily basis. DC- and LAPC-recipient mice exhibited less weight loss than the PBS control mice (Fig. 8 B). On day 8 after infection, all mice were euthanized and tissues were harvested for analysis. Consistent with the ex vivo experimental data described in Fig. 7, donor LAPCs augmented the Th2 effector T cell response in the DLNs without affecting either the Th1 or CTL responses in the DLNs and BAL (Fig. 8 C). Moreover, the data indicate that donor DCs specifically enhance antiinfluenza CTL responses in the DLNs and BAL (Fig. 8 C). DC- and LAPC-recipient

mice exhibited elevated serum IgG_{2a}, IgG_{2b}, IgG_1, and IgA production, relative to the PBS controls, with selectively enhanced IgE production in the LAPC-recipient mice (Fig. 8 D).

BAL cytokine production on day 8 after infection was examined by SearchLight proteome array analysis (Fig. 8 E). LAPC-recipient mice exhibited enhanced production of T2 cytokines, including IL-4, IL-5, and eotaxin, relative to DC recipients and PBS controls. Recently, Sun et al. (2009) have reported that IL-10 is produced in influenza virus–infected lung tissue exclusively by infiltrating virus-specific T1 effector T cells (Th1 cells and CTLs), with CTLs contributing a significant portion of the total IL-10 produced. In agreement, even though the data are not statistically significant for IL-10, we observe that DC-recipient mice have augmented CTL responses in their lungs, exhibiting elevated levels of IL-10 production compared with PBS controls (Fig. 8, C and E). However, LAPC-recipient mice do not show any difference in IL-10 production in BAL fluid compared with PBS controls. Because LAPCs do not affect the T1 effector T cell response (Th1 cells and CTLs) but contribute to the T2 effector T cell response (Th2 cells), the absence of any increase in IL-10 production in vivo might be anticipated. Neither T1 nor T2 cytokine production in the BAL on day 8 was significantly affected by DC transfer. Notably, LAPC-recipient mice showed exacerbated pulmonary pathology, as indicated by enhanced pulmonary eosinophilia (Fig. 8 F) and delayed viral clearance in the BAL (Fig. 8 G). Consistent with the observed enhanced CTL response, DC-recipient mice showed accelerated viral clearance compared with control mice, with no difference in pulmonary eosinophilia (Fig. 8, F and G).

DISCUSSION

In this study, we describe a novel leukocyte population, designated LAPCs. Phenotypic, genetic, and morphological characterization distinguished LAPCs from other mouse immune cells. Comparing the global gene expression profile of LAPCs with other immune cell types revealed that LAPCs are a distinct cell type, exhibiting a signature gene expression profile. Our studies with Rag-$1^{-/-}$, Flt3$L^{-/-}$, and IL-$15^{-/-}$ mice suggest that LAPCs follow a distinct developmental pathway from that of lymphocytes, DCs, and NK cells. Even though LAPCs express low levels of MHC-II before virus activation, the phenotypic characteristics of LAPCs do not conform with those of DC precursors, which express either CD11c or CD117 (c-kit; Naik et al., 2007). Two major DC precursor subtypes have been identified in mice, namely pro-DCs and pre-DCs, both of which have the potential to differentiate into three major DC subtypes (pDCs, $CD8\alpha^+$ cDCs, and $CD8\alpha^-$ cDCs). Pre-DCs are defined as $CD11c^+$MHC-II^- and pro-DCs are defined as $CD11c^-$ MHC-$II^-Ly6c^-CD117^+$. Given our FACS analysis of cell-surface markers and the gene expression data, LAPCs are a $CD11c^-Ly6c^+CD117^-$ population, from which we infer that LAPCs likely are not DC precursors. Further analysis of surface marker expression also distinguished LAPCs ($c\text{-}Kit^-CD34^-CD49b^-CD54^+Gr1^+Fc\varepsilon R\alpha1^-CD69^{low/-}$ $Thy1.2^-$) from either lymphoid or myeloid progenitor cells ($CD34^+$), basophils ($c\text{-}Kit^-CD49b^+CD54^+Gr1^-Fc\varepsilon R\alpha1^+$), and the recently indentified natural helper cells ($c\text{-}Kit^+CD69^+$ $Gr1^-Thy1.2^+$; Fig. 1 C and Fig. S1; Kondo et al., 1997, 2003; Sokol et al., 2009; Moro et al., 2010). Finally, LAPCs are BM-derived nongranular leukocytes with plasmacytoid morphology, likely of myeloid lineage. Neither influenza virus–activated nor IFN-γ– (10 ng/ml) and LPS-stimulated (1 μg/ml) LAPCs express iNOS, which further excludes the possibility that LAPCs are macrophages (Table S1 and unpublished data).

After pulmonary influenza A virus infection, LAPCs are detected in the lungs, likely a consequence of their migration out of the circulation mediated by CXCR3–CXCL10 interactions. In contrast to DCs, LAPCs exhibited delayed kinetics of migration from the lungs into the DLN, suggesting that they may have a distinct role in an immune response to virus infection. Notably, LAPCs were also identified in the DLNs of VACV- and CVB3-infected mice. Bréhin et al. (2008) have identified a similar cell type in lymphoid tissues from West Nile virus–infected BALB/c mice. This cell population, isolated from LNs on day 6 after infection, exhibited surface CD19 expression comparable to that of B cells. We have observed that, in contrast to LAPCs derived from naive mice, influenza virus–activated LAPCs exhibit only transient expression of CD19, on day 6 after infection, comparable to that of B cells (unpublished data).

As professional APCs in the immune system, DCs are responsible for initiating adaptive immune responses in lymphoid tissues (Banchereau et al., 2000). Certainly, during influenza virus infection, DCs play a key role in modulating adaptive T cell responses in both the lungs and the DLNs (Yoon et al., 2007; GeurtsvanKessel et al., 2008; McGill et al., 2008). Influenza A virus infection induces the maturation of DCs in the lungs, and DCs then migrate to the DLN to present viral Ags to virus-specific T cells (Yoon et al., 2007; GeurtsvanKessel et al., 2008). Additionally, a resident subset of DCs ($CD11b^-CD8\alpha^+$ DCs) in the DLN can also present viral Ags to $CD8^+$ T cells for up to 12 d after infection (Belz et al., 2004, 2007). However, it has been suggested that Ag presentation to $CD4^+$ T cells is restricted to the migrating DCs, whose accelerated migration is transient during the early phase of infection (before day 2), and these DCs have a limited half-life in the DLN (Legge and Braciale, 2003; GeurtsvanKessel et al., 2008). In this study, we also observed that DCs isolated from the DLN and spleen on day 8 after infection are capable of stimulating antiinfluenza CTL responses, presumably by presenting viral Ag to cognate $CD8^+$ T cells, with no evidence for Ag presentation to $CD4^+$ T cells (Fig. 7 C and Fig. 8 C).

Influenza A virus infection induces both T1 and T2 T cell responses (Carding et al., 1993; Graham et al., 1994; La Gruta et al., 2007). Antiinfluenza T1 immunity, implicated in viral clearance in infected lung tissues, is induced by DCs during the early phase of infection, around day 3 after infection, in the DLN (Carding et al., 1993; Cella et al., 2000; GeurtsvanKessel

et al., 2008). McGill et al. (2008) provided evidence that DCs also modulate the antiinfluenza CTL response in the lungs by TCR reengagement after the initial activation in the DLN. The predominant T2 response occurs later during infection, around day 7 after infection (Carding et al., 1993). This T2 response may play a role in down-regulating the strong T1

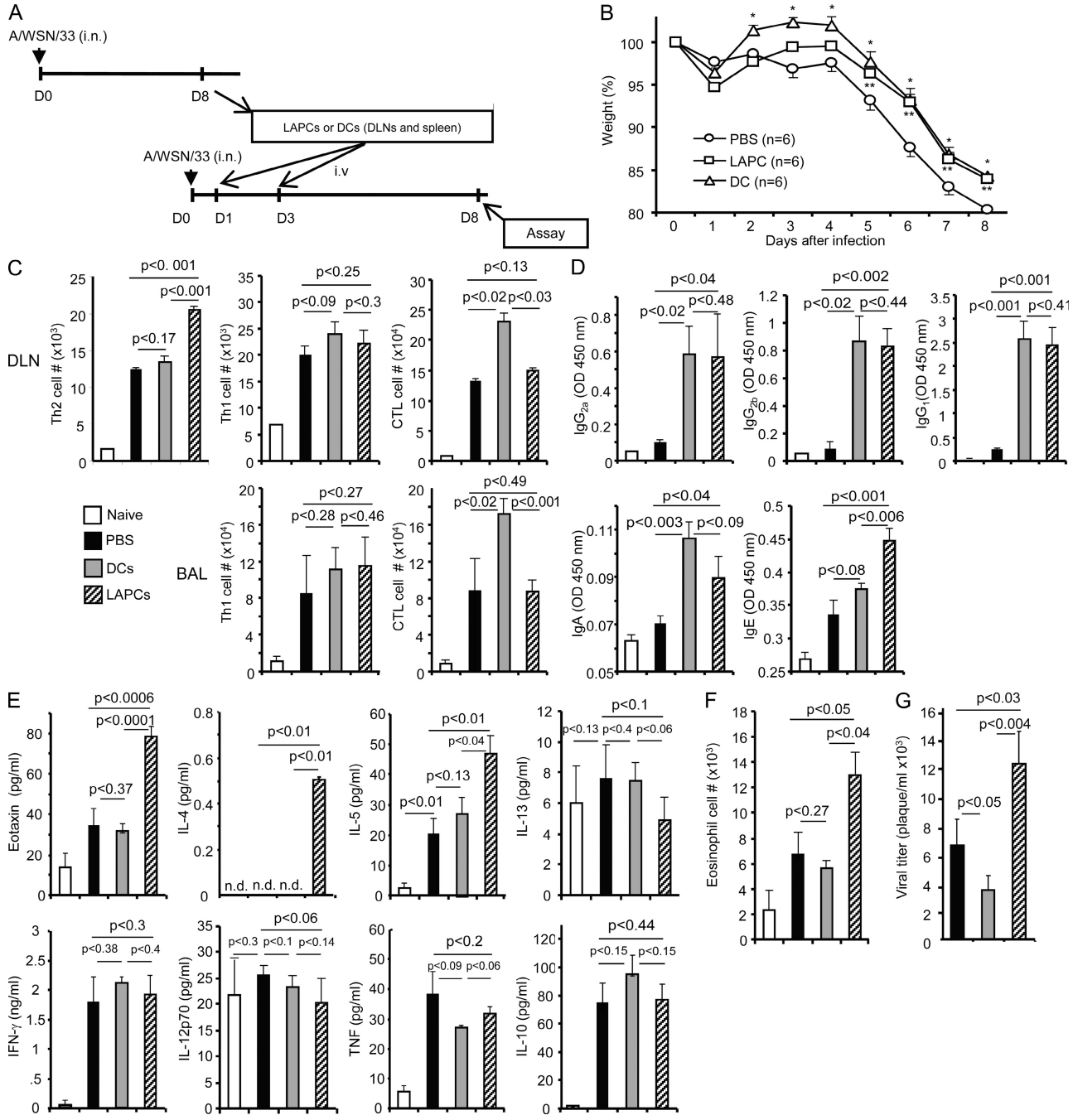

Figure 8. Influenza virus–activated LAPCs modulate antiinfluenza T2 immunity in vivo. (A) Schematic diagram for in vivo adoptive transfer experiments. (B) Weight loss was monitored daily and is shown as the percent weight loss relative to uninfected controls (means ± SEM). (D–G) On day 8 after infection, mice ($n = 6$ per each group) were sacrificed and effector T cell responses in the DLN and BAL (C), antiinfluenza humoral immune responses in serum (D), cytokine and chemokine levels in BAL fluid (E), pulmonary eosinophilia (F), and viral titers in BAL fluid (G) were determined as described in Materials and methods. Data representative of two independent experiments are shown as means ± SEM and were analyzed using a Student's *t* test. For cytokine and chemokine SearchLight proteome arrays, the values measured reflect dilution in 1 ml PBS to collect BAL fluid. The levels of detection for each cytokine and chemokine are described in Materials and methods. *, $P < 0.05$ for DC-recipient mice compared with PBS control mice; **, $P < 0.05$ for LAPC-recipient mice compared with PBS control mice.

response, mediated by IL-4– and IL-10–induced suppression of T1 effectors (Scott and Kaufmann, 1991; Romagnani, 1997). T2 responses invoke antiinfluenza Ig production, which provides a protective effect against secondary viral challenge (DeKruyff et al., 1993; Yamamoto et al., 1996; Renegar et al., 2004). T2 responses also contribute to immunopathology associated with primary influenza virus infection: a delayed viral clearance and conspicuous pulmonary eosinophilia are induced after adoptive transfer of antiinfluenza Th2 T cell clones (Graham et al., 1994), and T2 cytokines increase the severity of postinfectious encephalitis in mice exposed to influenza virus (Kaji et al., 2000). However, it is still unclear how this T2 immunity is regulated in influenza A virus–infected animals.

In the presence of the Th1-polarizing cytokine IL-12, a short duration of TCR stimulation is sufficient to induce Th1 polarization because IFN-γ production is rapidly induced. In contrast, a prolonged period of Ag stimulation has been suggested to be required to induce Th2 polarization, because the capacity to produce IL-4 and IL-13 is acquired slowly (Iezzi et al., 1999; Kaech et al., 2002). An unresolved issue has been how TCR signaling in $CD4^+$ T cells can be sustained for the extended time in the DLN of influenza virus–infected mice to successfully induce the antiviral Th2 response. In this study, we show that LAPCs can provide this signal to Ag-primed $CD4^+$ T cells at later phases of infection. In our study, influenza virus–activated LAPCs could induce Th2 polarization of Ag-primed $CD4^+$ T cells in an Ag-specific manner, from which we infer that serial stimulation of influenza virus–specific $CD4^+$ T cells by DCs and then LAPCs may occur to invoke a Th2 response. Although we cannot rule out the possibility that constitutive migratory DCs from infected lung tissue may also be involved in Th2 effector polarization in the DLN at later stages after infection, these cells comprise 2% of the total DCs (~140 cells) in the DLN after day 5 after infection (Legge and Braciale, 2003). Moreover, the data from our ex vivo study suggest that DCs isolated at a later phase after infection do not present viral Ag to cognate $CD4^+$ T cells for optimal Th2 polarization. Therefore, their relative contribution compared with LAPCs would appear to be minimal. This was further supported by our in vivo evidence showing that DCs isolated at later time points after infection from the DLN and spleen could only modulate the antiinfluenza CTL response in mice. Finally, recipient mice that received donor LAPCs but not DCs showed enhanced systemic and local antiinfluenza T2 immunity. Subsequently, these LAPC-recipient mice exhibited exacerbated pulmonary pathology, as indicated by augmented pulmonary eosinophilia and delayed viral clearance, suggesting that LAPCs, but not DCs, may play a pivotal role in modulating antiinfluenza virus T2 immunity in mice.

GATA-3 is a master regulator for Th2 lineage commitment (Zheng and Flavell, 1997). GATA-3 expression may be regulated either by IL-4–dependent or –independent mechanisms (Kubo, 2007). Our data show that LAPCs modulate GATA-3 expression through a soluble factor–independent mechanism, and demonstrate that cell–cell contact is critical for this LAPC-mediated regulation. Signals through OX40 or Notch have been implicated in IL-4–independent Th2 lineage commitment (Ito et al., 2005; Amsen et al., 2007). It is intriguing to speculate that LAPCs may provide Th2-polarizing signals through engagement of one of these receptors expressed on Ag-primed $CD4^+$ T cells coordinated with T cell receptor signaling. The underlying mechanism of LAPC-mediated Th2 polarization also remains to be addressed and is the subject of our ongoing investigations.

Collectively, our findings suggest that this novel leukocyte cell population may play a pivotal role in modulating T2 immunity against pulmonary influenza A virus infection, which is implicated in both immunoprotection and immunopathology. Moreover, our data suggest a more widespread involvement of these cells in different virus infections. Further insights into the in vivo function of LAPCs in different virus infections and in response to challenge with different pathogens and allergens may provide us with novel therapeutic targets for the treatment of different pathologies, including influenza A virus infection.

MATERIALS AND METHODS

Animals. C57BL/6J and OT-II Thy1.2 mice were bred and housed in the Toronto General Hospital animal facility. Rag-$1^{-/-}$, A/J, DBA/2J, and BALB/c mice were purchased from the Jackson Laboratory. Flt3$L^{-/-}$ and IL-$15^{-/-}$ mice were purchased from Taconic. OT-II Thy1.1/1.2 mice were provided by J. Gommerman (University of Toronto, Toronto, Canada). All mice were housed in a specific pathogen–free environment, and all experiments were approved by the Animal Care Committee of the Toronto General Research Institute.

Cell fractionation. Tissues (LNs, spleen, lungs, and thymus) were harvested and mechanically disrupted, followed by enzymatic digestion with collagenase D and DNase I (Roche). In brief, tissues were placed in cold PBS supplemented with 1 mM $MgCl_2$ and 1.8 mM $CaCl_2$ and compressed between two glass slides. These tissues were incubated at 37°C for 30 min with 1 mg/ml collagenase and 0.3 mg/ml DNase I. After incubation, DCs were dissociated from T cells by incubating with 1 mM EDTA for 10 min at room temperature. The cell suspension was filtered through a 70-μm mesh. RBCs were removed using ACK lysis buffer. PBMCs were collected from naive C57BL/6J mice. In brief, animals were sedated with isofluorane and up to 1 ml of peripheral blood was collected by cardiac puncture. PBMCs were isolated by Ficoll gradient centrifugation at 800 *g* for 20 min, and the PBMC layer was washed in cold PBS. BM cells were obtained from mice by flushing the marrow from femurs into cold PBS. RBCs were removed using ACK lysis buffer.

Virus infections. 8–12-wk-old mice were anesthetized by intraperitoneal inoculation with a mixture of ketamine and xylazine, and infected either by intranasal instillation with 50 μl PBS containing A/WSN/33 (H1N1) influenza virus (a gift from G. Whittaker, Cornell University, Ithaca, NY) or the recombinant strain Western Reserve VACV (a gift from G. McFadden, University of Florida, Gainesville, FL), or for CVB3 infection, by intraperitoneal injection with 100 μl PBS containing CVB3 (a gift from P.P. Liu, University Health Network, Toronto, Canada). At the times after infection indicated in the figures, mice were sacrificed by cervical dislocation and the mediastinal, inguinal, and axillary LNs, lungs, and spleens were harvested and processed as previously described.

Antibody staining and flow cytometry. Fluorochrome-labeled mAbs specific for CD4 (GK1.5), CD8α (53-6.7), CD11b (M1/70), CD11c (N418), CD19 (MB19-1), CD34 (RAM34), CD40 (1C10), CD44 (1M7), B220/CD45R (RA3-6B2), CD49b (DX5), CD62L (MEL-14), CD69 (H1.2F3),

CD80 (16-10A1), CD86 (GL1), CD117 (2B8), CD122 (5H4), NK1.1 (PK136), F4/80 (BM8), Gr1 (RB6-8C5), TCRβ (H57-597), Thy1.1 (HIS51), Thy1.2 (53-2.1), IL-2 (JES6-5H4), IL-4 (11B11), IL-10 (JES5-16E3), IFN-γ (XMG1.2), and MHC-II (I-A/E; M5/114.15.2) were obtained from eBioscience. A FITC-conjugated mAb to mPDCA-1 (JF05-1C2.4.1) was purchased from Miltenyi Biotec. Anti-CD79b (HM79b), -CD138 (281-2), -TCRγδ (GL3), and –GATA-3 (L50-823) mAbs were purchased from BD. A CXCR3 (220803)-specific mAb was obtained from R&D Systems, and a mAb specific for DEC 205 (NLDC-145) was purchased from BMA Biomedical AG. Flow cytometry was performed on FACSCalibur and FACSAria instruments (BD), with optimal compensation set for four-color staining. The data were analyzed using FlowJo software (Tree Star, Inc.).

To examine cytokine production, cells were restimulated with 50 ng/ml PMA, 500 ng/ml ionomycin (Sigma Aldrich), and GolgiPlug (BD) for 4 h, washed with FACS buffer (PBS supplemented with 2% FBS), and surface stained with the appropriate identifier fluorochrome-conjugated mAbs. After fixation and permeabilization with Cytofix/Cytoperm buffer (BD), intracellular staining was performed using mAbs for each cytokine followed by FACS analysis.

Sample processing and microarray analysis for LAPCs. Groups of mice were either mock (PBS)-infected ($n = 10$) or infected with influenza virus (500 PFU; $n = 5$) by intranasal instillation and sacrificed on day 8 after infection, and DLNs were harvested. LAPCs were sorted by FACS and total RNA was prepared using either the RNeasy Mini or Micro Kit (QIAGEN). RNA was processed using a two-round RNA amplification protocol described by Affymetrix (GeneChip Expression Manual Small Sample 2). The preparation of cDNA from RNA, sample hybridization, and scanning of the GeneChip Mouse Genome 430 2.0 Array (Affymetrix) were performed at the Center for Applied Genomics Microarray Facility (Hospital for Sick Children, Toronto, Canada) in accordance with the procedures established by Affymetrix. Microarray data for LAPCs have been deposited in the Gene Expression Omnibus under accession no. GSE17726.

Data processing and integration with public data. Raw expression data for LAPCs were imported into R and Bioconductor for initial quality assessment using the arrayQuality package. Once satisfied that there were no technical issues, LAPC data were combined with several publicly available datasets of mouse immune system cell types. Included were mouse splenic gene expression datasets performed on the GeneChip Mouse Genome 430 2.0 Array by Robbins et al. (2008). Cell types included $CD11b^+$ DCs ($n = 2$), $CD8\alpha^+$ cDCs ($n = 2$), pDCs ($n = 2$), B cells ($n = 3$), NK cells ($n = 2$), and $CD8^+$ T cells ($n = 2$). These data have been deposited in the Gene Expression Omnibus under accession no. GSE9810. In addition, macrophage gene expression data from young mice ($n = 3$; Chelvarajan et al., 2006) were collected from the National Cancer Institute caArray (http://caarray.nci.nih.gov/) along with control $CD4^+$ T cell gene expression data ($n = 2$; microarray data have been deposited in the Gene Expression Omnibus under accession nos. GSM44979 and GSM44982; Fontenot et al., 2005). Finally, we included two samples of mast cells from a gene expression dataset that is part of the mouse gene atlas project (http://biogps.gnf.org/#goto=welcome; microarray data have been deposited in the Gene Expression Omnibus under accession nos. GSM258711 and GSM258712) and two samples of granulocytes from another dataset (microarray data have been deposited in the Gene Expression Omnibus under accession nos. GSM149595 and GSM149596). Gene expression data from all cel files were imported into GeneSpring analysis software (version 10; Agilent Technologies). All data were preprocessed using the RMA algorithm (Irizarry et al., 2003). Data were further normalized to the median expression measure for each gene across all samples and logged (base 2).

As a starting point, probes used in a previous paper (Table 2 in Robbins et al. [2008]) were used as a cassette of control genes to compare expression across all cell types. In addition to this, several other probes of interest were also included (Table S1).

Gene expression data were then subjected to further analysis. In the initial stage of analysis, the similarity of LAPCs to other immune cell types was determined. First, probes on the array that were greater than twofold different between LAPCs isolated from PBS- and influenza A virus–infected mice were removed, leaving 36,290 probes. This was done to only look at those probes that did not vary greatly between the LAPCs. The probes were then clustered using an unsupervised two-way hierarchical average linkage clustering algorithm with a Pearson centered distance metric. The resulting tree was examined for trends (Fig. 2).

In the second stage of analysis, a potential set of marker genes for LAPCs was sought. First, probes with consistently low signal measurements were removed to decrease unnecessary noise. Each probe was averaged across replicates for each cell type, and only those probes with an intensity measurement greater than the 30th percentile of all probes on a single chip in at least one of the cell types was allowed to pass through to the next stage of analysis. The resulting 36,589 probes were subjected to analysis of variance with a multiple testing Benjamini and Hochberg correction at the $P < 0.05$ significance level. 30,072 probes were found to be significantly different among all 11 cell types. To identify LAPC-specific markers, only those probes that identified expressed genes that displayed a 10-fold difference between LAPCs and any other immune cell lineage in at least 5 out of the 10 possible comparisons were allowed. This final list of 279 expressed gene probes was examined by hand to find the best candidate unique genes, with the criterion that the genes are only expressed by LAPCs based on an Affymetrix intensity value >100. The data are presented as a heat map representing relative expression values as obtained after $\log_{10}$ transformation and median centering of the values across cell samples for each gene (Fig. S2).

Morphological analysis. For cytological analysis, FACS-sorted cells from either naive or influenza virus–infected mice were cytocentrifuged (600 rpm for 1 min) onto microscope slides and stained with modified Wright-Giemsa, and their morphology was examined by light microscopy (Axioskop 2; Carl Zeiss, Inc.).

Transmission electron microscopy. To visualize cells at the ultrastructure level, cells were fixed in 1% glutaraldehyde, 4% paraformaldehyde in 0.1 M PBS buffer, pH 7.2 (overnight at 4°C), washed, and postfixed in 1% OsO_4 for 1 h. After rinsing with 0.1 M PBS buffer, pH 7.2, dehydration steps were followed through graded ethanol series. Cells were embedded in EPON 812 (Ted Pella), polymerized for 48 h at 60°C. Ultrathin sections (80 nm) were collected onto 300 mesh copper grids, stained with 5% uranyl acetate and 0.03% lead citrate. Sections were visualized using a transmission electron microscope (H7000; Hitachi) operating at 75 kV. The images were captured using a digital 16-bit AMT camera. Representative images were selected and shown.

In vivo Ag uptake assay. Mice were anesthetized as described in Virus infections and infected by intranasal instillation with 50 µl PBS containing 500 PFU of A/WSN/33 influenza virus either with or without FITC-dextran (40 kD, 1 mg/ml). On day 3 after infection, mice were sacrificed and cells were collected from lungs. FACS analysis was performed to examine the percent population of $FITC^+$ cells, gating on T cells ($TCR\beta^+$), pDCs ($mPDCA\text{-}1^+CD11c^{int}$), and LAPCs ($mPDCA\text{-}1^+CD11c^-TCR\beta^-B220^-$) in lungs.

In vivo migration assay. LAPC migration was examined as previously described (Legge and Braciale, 2003), with minor modifications. In brief, mice were anesthetized as described in Virus infections and infected with 50 µl PBS containing 500 PFU of A/WSN/33 influenza virus. On day 4 after infection, either 8 mM CFSE diluted in IMDM or medium alone was instilled intranasally (50 µl/mouse) into individual mice to label all lung-infiltrated cells, including LAPCs. 7 h after labeling, selected mice were sacrificed to examine the efficiency of in vivo CFSE labeling using FACS analysis. On day 8 after infection, mice were sacrificed, the DLNs and spleens were harvested, and the percent population of $CFSE^+$ cells, gating on LAPCs, was examined by FACS analysis.

DEAD assay. C57BL/6J mice were infected by intranasal instillation with 500 PFU of either A/WSN/33 or A/WSN/OVA(II) virus. A/WSN/OVA(II) virus was provided by D. Topham (University of Rochester, Rochester, NY; Chapman et al., 2005). DCs (pDCs, mPDCA-1$^+$CD11c^{int}; cDCs, CD11c^{high}B220$^-$) and LAPCs were sorted from the DLNs on days 3 and 8 after infection, respectively, by FACS. To optimize culture condition, sorted APCs were co-cultured with naive OT-II T cells with various APC/T cell ratios (1:10, 1:4, 1:3, and 1:2 ratios were tested). To examine for their ability to activate OVA-specific OT-II T cells, at 48, 72, and 96 h after in vitro co-culture, samples were harvested and T cell activation was examined by intracellular IL-2 staining for T cells. Finally, a 1:2 ratio between APCs/T cells (5×10^4 APCs/well; 10^5 OT-II T cells/well) was selected as the optimized culture conditions. At 96 h after incubation, cells were either stimulated with 50 ng/ml PMA, 500 ng/ml ionomycin, and GolgiPlug (BD) for 4 h, or were treated with GolgiPlug only for 4 h. Cells were collected, washed, and surface stained with fluorochrome-conjugated anti-CD4 and Thy1.2 mAbs. After fixation and permeabilization, intracellular staining was performed using a PE-conjugated IL-2–specific mAb. Data are presented as the percent population of IL-2–positive cells in total OT-II.

In vivo tracking assay. Mice ($n = 10$) were infected by intranasal instillation with 500 PFU of influenza virus, and activated LAPCs were then isolated from the DLNs on day 6 after infection. FACS-sorted cells were stained with CFSE (Invitrogen) according to the manufacturer's instructions, and CFSE-labeled LAPCs were adoptively transferred by i.v. injection (10^6 cells/mouse) into recipient influenza virus–infected mice ($n = 2$; 500 PFU) on day 6 after infection. 24 h after transfer, the mice were euthanized and the DLNs were harvested and frozen in Tissue-Tek solution (Sakura). Tissues were cryosectioned (20 μm) and thin-section slides were prepared. Slides were warmed to room temperature and washed in PBS, and the sections were fixed in 1:1 methanol/acetone at −20°C for 15 min. The thin sections were then dried and frozen at −70°C for 30 min. Tissue sections were washed in PBS and blocked with 0.2% gelatin at 4°C overnight. Sections were stained with anti-B220–APC antibody (1:50; BD). Slides were examined by a laser scanning confocal microscope (FluoView 1000; Olympus). Final image processing was performed using the FluoView viewer (version 1.7.a; Olympus).

CD4$^+$ T cell isolation. LN-derived CD4$^+$ T cells were isolated from either naive OT-II Thy1.2 or OT-II Thy1.1/1.2 mice by depletion of non-CD4$^+$ T cells (negative selection) using a CD4$^+$ T cell isolation kit (Miltenyi Biotec). To isolate in vivo Ag-primed OT-II T cells, purified Thy1.1$^+$ OT-II T cells were transferred into Thy1.2$^+$ C57BL/6J mice by i.v. injection. 24 h after adoptive transfer, recipient mice were infected intranasally with 500 PFU of A/WSN/OVA(II) virus. On day 5 after infection, mice were sacrificed and their DLNs were harvested. Thy1.1$^+$CD4$^+$ cells were isolated from the DLNs by FACS sorting. The isolated CD4$^+$ T cells were subjected to FACS analysis to confirm purity (MACS, ∼90%; FACS, ≥97%).

Transwell experiment. To examine whether LAPCs induce effector T cell generation through direct cell contact or through release of soluble factors, Transwell experiments were performed. In vivo primed OT-II T cells were added to individual wells (10^5 cells/well) of a 96-well Transwell plate in the lower chamber and influenza virus–activated LAPCs were introduced into individual wells (5×10^4 cells/well) in the upper chamber. Cells were separated with a 0.4-μm pore membrane (Costar; Corning), which allows diffusion of small molecules, such as cytokines, but not cells. All experiments were performed in triplicate. After 24 h, T cells are harvested from the lower compartments and assayed for IL-4 and IFN-γ production by FACS analysis.

Adoptive transfer of influenza virus–activated LAPCs and DCs. Mice were infected with 300 PFU of A/WSN/33 virus as described. On day 8 after infection, mice were sacrificed and influenza virus–activated LAPCs or DCs were harvested from the DLNs and spleens by FACS sorting. The isolated cells were subjected to FACS analysis to confirm purity (≥98%). 200 μl of sterile PBS buffer either with or without sorted cells was injected into A/WSN/33 virus–infected (300 PFU) recipient mice on days 1 (3×10^5 cells/mouse) and 3 (5×10^5 cells/mouse) after infection by i.v. injection. Weight loss was monitored until day 8 after infection and shown as the percent weight loss relative to day 0 control mice.

Influenza virus titration. Viral titers in BAL fluid were determined using a Madin-Darby canine kidney (MDCK) cell plaque assay. On day 8 after infection, mice were euthanized and BAL fluid was harvested. MDCK cells were seeded in MEM in individual wells of 6-well plates until confluent. 10-fold serial dilutions of BAL fluid were prepared in serum-free MEM. A total of 200 μl of each dilution was added to individual wells (in duplicate) for 30 min at 37°C. Cells were then overlaid with 3 ml of 1× MEM containing 0.65% agarose, antibiotics, L-glutamine, and 1 μg/ml trypsin. 40 h after incubation at 37°C, cells were fixed with 2 ml Carnoy's fixative (methanol/glacial acetic acid, 3:1) for 30 min. The agarose overlay was then removed and fixed monolayers were stained by adding crystal violet prepared in 20% ethanol to permit visualization of viral plaques for counting.

Influenza virus–specific antibody ELISA. Serum was collected from either naive mice or influenza virus–infected mice on day 8 after infection and examined for influenza virus–specific antibody responses by ELISA. In brief, 96-well plates were coated overnight at 4°C with 100 μl (10^6 PFU) of heat-inactivated (58°C) A/WSN/33 influenza virus. The plates were washed twice with PBS supplemented with 0.05% Tween-20 (PBST) and incubated with 100 μl of 2% BSA in PBST for 1 h at room temperature. After washing the plates with PBST, 100 μl of diluted serum was added to each well, in duplicate, and incubated for 2 h at room temperature. Bound antibodies were detected by the incubation of horseradish peroxidase–conjugated anti–mouse IgG1 (1:1,000), IgG2a (1:1,000; BD), IgG2b (1:1,000), IgA (1:8,000; SouthernBiotech), or IgE (1:1,000; AbD Serotec) antibodies at room temperature. After 1 h, the plates were washed with PBST, and 100 μl of 3,3′,5,5′-tetramethylbenzidine substrate solution (Sigma-Aldrich) was added into each well and incubated for 30 min. The enzyme reaction was stopped by adding 100 μl of 2N H_2SO_4 and OD values were determined at 450 nm using a plate reader (SpectraMax 384 Plus UV-VIS; MDS Analytical Technologies).

Determination of cell numbers and cytokine levels in BAL. Mice were sacrificed at the times after infection indicated in the figures. Lungs were excised together with trachea and flushed with 1 ml PBS using a blunted 23-gauge needle inserted into the trachea. Cells were collected by centrifugation at 400 *g* for 5 min. The supernatants were collected and stored frozen at −80°C until analyzed for cytokine and chemokine expression using proteome arrays (SearchLight; Aushon BioSystems). The limits of detection of each cytokine and chemokine in this assay are as follows: eotaxin, 0.1–200 pg/ml; IFN-γ, 3.9–8,000 pg/ml; IL-5, 0.8–1,600 pg/ml; IL-4, 0.4–800 pg/ml; IL-12p70, 0.4–800 pg/ml; IL-13, 0.8–1,600 pg/ml; TNF, 1.6–3,200 pg/ml; IL-10, 0.8–1,600 pg/ml; and CXCL10/IP-10, 0.4–800 pg/ml. The cells were resuspended and RBCs were lysed with ACK lysis buffer. Cells were washed twice with PBS and resuspended in FACS buffer. Cell numbers were counted using a hemocytometer. Cells were stained with a panel of fluorochrome-conjugated mAbs and analyzed using a FACSCalibur.

[^{3}H]Thymidine incorporation assay. C57BL/6J mice were infected by intranasal instillation with either 500 PFU of A/WSN/33 or A/WSN/OVA(II) virus. DCs (CD11c$^+$) were isolated from the DLNs on day 3 after infection and from the LAPCs on day 8 after infection by FACS sorting. Isolated APCs were γ-irradiated (2,000 rads) and incubated together with naive OT-II T cells in 96-well plates (10^5 APCs/well; 5×10^4 OT-II T cells/well). As positive controls, OT-II T cells were incubated together with $OVA_{323–339}$ peptide pulsed γ-irradiated APCs (DCs or LAPCs). 78 h after incubation, 1 μCi [^{3}H]thymidine was added to each well and cells were incubated for a further 18 h. [^{3}H]Thymidine incorporation was analyzed with a β-scintillation counter.

Statistical analysis. Data were analyzed by an unpaired two-tailed Student's *t* test unless otherwise noted in the figure legends. $P < 0.05$ was considered significant. Data are expressed as either means ± SD or SEM.

Online supplemental material. Fig. S1 shows the differences between LAPCs and basophils in terms of surface marker expression. Fig. S2 describes a potential set of marker genes for LAPCs. Fig. S3 shows LAPC abundance in LNs and spleens in different mouse strains. Fig. S4 shows CXCL10 production in influenza virus–infected lungs and CXCR3 expression on LAPCs. Fig. S5 shows the in vivo Ag-presenting capacity of LAPCs by a [^{3}H]thymidine incorporation assay. Fig. S6 shows that in Flt3L$^{-/-}$ mice influenza virus–activated LAPCs present viral Ag to cognate CD4$^+$ T cells, independent of DCs. Fig. S7 shows that influenza virus–activated LAPCs induce Th2 effector cell polarization of in vivo Ag-primed CD4$^+$ T cells. Table S1 shows gene expression profiles of lineage markers and selected genes for multiple immune cells, including LAPCs. Online supplemental material is available at http://www.jem.org/cgi/content/full/jem.20091373/DC1.

The authors are also grateful to D. Burke, Dr. R. Rahbar, and Dr. J. Gommerman for their helpful discussions.

These studies were supported by a Canadian Institutes of Health Research grant (MOP-15094 to E.N. Fish). J.K. Yoo was supported by a Connaught Scholarship and an Ontario Graduate Scholarship in Science and Technology. E.N. Fish is the recipient of a Tier 1 Canada Research Chair.

The authors have no conflicting financial interests.

Submitted: 23 June 2009
Accepted: 12 May 2010

REFERENCES

Amsen, D., A. Antov, D. Jankovic, A. Sher, F. Radtke, A. Souabni, M. Busslinger, B. McCright, T. Gridley, and R.A. Flavell. 2007. Direct regulation of Gata3 expression determines the T helper differentiation potential of Notch. *Immunity*. 27:89–99. doi:10.1016/j.immuni.2007.05.021

Baboonian, C., M.J. Davies, J.C. Booth, and W.J. McKenna. 1997. Coxsackie B viruses and human heart disease. *Curr. Top. Microbiol. Immunol.* 223:31–52.

Banchereau, J., F. Briere, C. Caux, J. Davoust, S. Lebecque, Y.J. Liu, B. Pulendran, and K. Palucka. 2000. Immunobiology of dendritic cells. *Annu. Rev. Immunol.* 18:767–811. doi:10.1146/annurev.immunol.18.1.767

Becker-Herman, S., F. Lantner, and I. Shachar. 2002. Id2 negatively regulates B cell differentiation in the spleen. *J. Immunol.* 168:5507–5513.

Belz, G.T., C.M. Smith, L. Kleinert, P. Reading, A. Brooks, K. Shortman, F.R. Carbone, and W.R. Heath. 2004. Distinct migrating and nonmigrating dendritic cell populations are involved in MHC class I-restricted antigen presentation after lung infection with virus. *Proc. Natl. Acad. Sci. USA*. 101:8670–8675. doi:10.1073/pnas.0402644101

Belz, G.T., S. Bedoui, F. Kupresanin, F.R. Carbone, and W.R. Heath. 2007. Minimal activation of memory CD8+ T cell by tissue-derived dendritic cells favors the stimulation of naive CD8+ T cells. *Nat. Immunol.* 8:1060–1066. doi:10.1038/ni1505

Blasius, A.L., E. Giurisato, M. Cella, R.D. Schreiber, A.S. Shaw, and M. Colonna. 2006. Bone marrow stromal cell antigen 2 is a specific marker of type I IFN-producing cells in the naive mouse, but a promiscuous cell surface antigen following IFN stimulation. *J. Immunol.* 177:3260–3265.

Bréhin, A.C., J. Mouriès, M.P. Frenkiel, G. Dadaglio, P. Desprès, M. Lafon, and T. Couderc. 2008. Dynamics of immune cell recruitment during West Nile encephalitis and identification of a new CD19+B220−BST-2+ leukocyte population. *J. Immunol.* 180:6760–6767.

Buchweitz, J.P., J.R. Harkema, and N.E. Kaminski. 2007. Time-dependent airway epithelial and inflammatory cell responses induced by influenza virus A/PR/8/34 in C57BL/6 mice. *Toxicol. Pathol.* 35:424–435. doi:10.1080/01926230701302558

Carding, S.R., W. Allan, A. McMickle, and P.C. Doherty. 1993. Activation of cytokine genes in T cells during primary and secondary murine influenza pneumonia. *J. Exp. Med.* 177:475–482. doi:10.1084/jem.177.2.475

Cella, M., F. Facchetti, A. Lanzavecchia, and M. Colonna. 2000. Plasmacytoid dendritic cells activated by influenza virus and CD40L drive a potent TH1 polarization. *Nat. Immunol.* 1:305–310. doi:10.1038/79747

Chapman, T.J., M.R. Castrucci, R.C. Padrick, L.M. Bradley, and D.J. Topham. 2005. Antigen-specific and non-specific CD4+ T cell recruitment and proliferation during influenza infection. *Virology*. 340:296–306. doi:10.1016/j.virol.2005.06.023

Chelvarajan, R.L., Y. Liu, D. Popa, M.L. Getchell, T.V. Getchell, A.J. Stromberg, and S. Bondada. 2006. Molecular basis of age-associated cytokine dysregulation in LPS-stimulated macrophages. *J. Leukoc. Biol.* 79:1314–1327. doi:10.1189/jlb.0106024

Clements, M.L., R.F. Betts, E.L. Tierney, and B.R. Murphy. 1986. Serum and nasal wash antibodies associated with resistance to experimental challenge with influenza A wild-type virus. *J. Clin. Microbiol.* 24:157–160.

Corcoran, L., I. Ferrero, D. Vremec, K. Lucas, J. Waithman, M. O'Keeffe, L. Wu, A. Wilson, and K. Shortman. 2003. The lymphoid past of mouse plasmacytoid cells and thymic dendritic cells. *J. Immunol.* 170:4926–4932.

Cox, N.J., and K. Subbarao. 2000. Global epidemiology of influenza: past and present. *Annu. Rev. Med.* 51:407–421. doi:10.1146/annurev.med.51.1.407

Dawson, T.C., M.A. Beck, W.A. Kuziel, F. Henderson, and N. Maeda. 2000. Contrasting effects of CCR5 and CCR2 deficiency in the pulmonary inflammatory response to influenza A virus. *Am. J. Pathol.* 156:1951–1959.

DeKruyff, R.H., L.V. Rizzo, and D.T. Umetsu. 1993. Induction of immunoglobulin synthesis by CD4+ T cell clones. *Semin. Immunol.* 5:421–430. doi:10.1006/smim.1993.1048

Doherty, P.C., S.J. Turner, R.G. Webby, and P.G. Thomas. 2006. Influenza and the challenge for immunology. *Nat. Immunol.* 7:449–455. doi:10.1038/ni1343

Fleming, T.J., M.L. Fleming, and T.R. Malek. 1993. Selective expression of Ly-6G on myeloid lineage cells in mouse bone marrow. RB6-8C5 mAb to granulocyte-differentiation antigen (Gr-1) detects members of the Ly-6 family. *J. Immunol.* 151:2399–2408.

Fontenot, J.D., J.P. Rasmussen, L.M. Williams, J.L. Dooley, A.G. Farr, and A.Y. Rudensky. 2005. Regulatory T cell lineage specification by the forkhead transcription factor foxp3. *Immunity*. 22:329–341. doi:10.1016/j.immuni.2005.01.016

Fort, M.M., J. Cheung, D. Yen, J. Li, S.M. Zurawski, S. Lo, S. Menon, T. Clifford, B. Hunte, R. Lesley, et al. 2001. IL-25 induces IL-4, IL-5, and IL-13 and Th2-associated pathologies in vivo. *Immunity*. 15:985–995. doi:10.1016/S1074-7613(01)00243-6

Garcon, N.M., J. Groothuis, S. Brown, B. Lauer, P. Pietrobon, and H.R. Six. 1990. Serum IgG subclass antibody responses in children vaccinated with influenza virus antigens by live attenuated or inactivated vaccines. *Antiviral Res.* 14:109–116. doi:10.1016/0166-3542(90)90048-C

GeurtsvanKessel, C.H., M.A. Willart, L.S. van Rijt, F. Muskens, M. Kool, C. Baas, K. Thielemans, C. Bennett, B.E. Clausen, H.C. Hoogsteden, et al. 2008. Clearance of influenza virus from the lung depends on migratory langerin$^+$CD11b$^-$ but not plasmacytoid dendritic cells. *J. Exp. Med.* 205:1621–1634. doi:10.1084/jem.20071365

Graham, M.B., V.L. Braciale, and T.J. Braciale. 1994. Influenza virus–specific CD4$^+$ T helper type 2 T lymphocytes do not promote recovery from experimental virus infection. *J. Exp. Med.* 180:1273–1282. doi:10.1084/jem.180.4.1273

Hacker, C., R.D. Kirsch, X.S. Ju, T. Hieronymus, T.C. Gust, C. Kuhl, T. Jorgas, S.M. Kurz, S. Rose-John, Y. Yokota, and M. Zenke. 2003. Transcriptional profiling identifies Id2 function in dendritic cell development. *Nat. Immunol.* 4:380–386. doi:10.1038/ni903

Hurst, S.D., T. Muchamuel, D.M. Gorman, J.M. Gilbert, T. Clifford, S. Kwan, S. Menon, B. Seymour, C. Jackson, T.T. Kung, et al. 2002. New IL-17 family members promote Th1 or Th2 responses in the lung: in vivo function of the novel cytokine IL-25. *J. Immunol.* 169:443–453.

Iezzi, G., E. Scotet, D. Scheidegger, and A. Lanzavecchia. 1999. The interplay between the duration of TCR and cytokine signaling determines T cell polarization. *Eur. J. Immunol.* 29:4092–4101. doi:10.1002/(SICI)1521-4141(199912)29:12<4092::AID-IMMU4092>3.0.CO;2-A

Irizarry, R.A., B. Hobbs, F. Collin, Y.D. Beazer-Barclay, K.J. Antonellis, U. Scherf, and T.P. Speed. 2003. Exploration, normalization, and summaries of high density oligonucleotide array probe level data. *Biostatistics*. 4:249–264. doi:10.1093/biostatistics/4.2.249

Ito, T., Y.H. Wang, O. Duramad, T. Hori, G.J. Delespesse, N. Watanabe, F.X. Qin, Z. Yao, W. Cao, and Y.J. Liu. 2005. TSLP-activated dendritic cells induce an inflammatory T helper type 2 cell response through OX40 ligand. *J. Exp. Med.* 202:1213–1223. doi:10.1084/jem.20051135

Kaech, S.M., E.J. Wherry, and R. Ahmed. 2002. Effector and memory T-cell differentiation: implications for vaccine development. *Nat. Rev. Immunol.* 2:251–262. doi:10.1038/nri778

Kaji, M., M. Kobayashi, R.B. Pollard, and F. Suzuki. 2000. Influence of type 2 T cell responses on the severity of encephalitis associated with influenza virus infection. *J. Leukoc. Biol.* 68:180–186.

Kennedy, M.K., M. Glaccum, S.N. Brown, E.A. Butz, J.L. Viney, M. Embers, N. Matsuki, K. Charrier, L. Sedger, C.R. Willis, et al. 2000. Reversible defects in natural killer and memory CD8 T cell lineages in interleukin 15–deficient mice. *J. Exp. Med.* 191:771–780. doi:10.1084/jem.191.5.771

Kondo, M., I.L. Weissman, and K. Akashi. 1997. Identification of clonogenic common lymphoid progenitors in mouse bone marrow. *Cell.* 91:661–672. doi:10.1016/S0092-8674(00)80453-5

Kondo, M., A.J. Wagers, M.G. Manz, S.S. Prohaska, D.C. Scherer, G.F. Beilhack, J.A. Shizuru, and I.L. Weissman. 2003. Biology of hematopoietic stem cells and progenitors: implications for clinical application. *Annu. Rev. Immunol.* 21:759–806. doi:10.1146/annurev.immunol.21.120601.141007

Kubo, M. 2007. Notch: filling a hole in T helper 2 cell differentiation. *Immunity.* 27:3–5. doi:10.1016/j.immuni.2007.07.005

La Gruta, N.L., K. Kedzierska, J. Stambas, and P.C. Doherty. 2007. A question of self-preservation: immunopathology in influenza virus infection. *Immunol. Cell Biol.* 85:85–92. doi:10.1038/sj.icb.7100026

Legge, K.L., and T.J. Braciale. 2003. Accelerated migration of respiratory dendritic cells to the regional lymph nodes is limited to the early phase of pulmonary infection. *Immunity.* 18:265–277. doi:10.1016/S1074-7613(03)00023-2

Maiti, A., G. Maki, and P. Johnson. 1998. TNF-alpha induction of CD44-mediated leukocyte adhesion by sulfation. *Science.* 282:941–943. doi:10.1126/science.282.5390.941

Marshall, D., R. Sealy, M. Sangster, and C. Coleclough. 1999. TH cells primed during influenza virus infection provide help for qualitatively distinct antibody responses to subsequent immunization. *J. Immunol.* 163:4673–4682.

McGill, J., N. Van Rooijen, and K.L. Legge. 2008. Protective influenza-specific CD8 T cell responses require interactions with dendritic cells in the lungs. *J. Exp. Med.* 205:1635–1646. doi:10.1084/jem.20080314

McKenna, H.J., K.L. Stocking, R.E. Miller, K. Brasel, T. De Smedt, E. Maraskovsky, C.R. Maliszewski, D.H. Lynch, J. Smith, B. Pulendran, et al. 2000. Mice lacking flt3 ligand have deficient hematopoiesis affecting hematopoietic progenitor cells, dendritic cells, and natural killer cells. *Blood.* 95:3489–3497.

Moro, K., T. Yamada, M. Tanabe, T. Takeuchi, T. Ikawa, H. Kawamoto, J. Furusawa, M. Ohtani, H. Fujii, and S. Koyasu. 2010. Innate production of T(H)2 cytokines by adipose tissue-associated c-Kit(+)Sca-1(+) lymphoid cells. *Nature.* 463:540–544. doi:10.1038/nature08636

Naik, S.H., P. Sathe, H.Y. Park, D. Metcalf, A.I. Proietto, A. Dakic, S. Carotta, M. O'Keeffe, M. Bahlo, A. Papenfuss, et al. 2007. Development of plasmacytoid and conventional dendritic cell subtypes from single precursor cells derived in vitro and in vivo. *Nat. Immunol.* 8:1217–1226. doi:10.1038/ni1522

Oliver, A.M., F. Martin, and J.F. Kearney. 1997. Mouse CD38 is down-regulated on germinal center B cells and mature plasma cells. *J. Immunol.* 158:1108–1115.

Palladino, G., K. Mozdzanowska, G. Washko, and W. Gerhard. 1995. Virus-neutralizing antibodies of immunoglobulin G (IgG) but not of IgM or IgA isotypes can cure influenza virus pneumonia in SCID mice. *J. Virol.* 69:2075–2081.

Renegar, K.B., P.A. Small Jr., L.G. Boykins, and P.F. Wright. 2004. Role of IgA versus IgG in the control of influenza viral infection in the murine respiratory tract. *J. Immunol.* 173:1978–1986.

Robbins, S.H., T. Walzer, D. Dembélé, C. Thibault, A. Defays, G. Bessou, H. Xu, E. Vivier, M. Sellars, P. Pierre, et al. 2008. Novel insights into the relationships between dendritic cell subsets in human and mouse revealed by genome-wide expression profiling. *Genome Biol.* 9:R17. doi:10.1186/gb-2008-9-1-r17

Roboz, G.J., and S. Rafii. 1999. Interleukin-5 and the regulation of eosinophil production. *Curr. Opin. Hematol.* 6:164–168. doi:10.1097/00062752-199905000-00007

Romagnani, S. 1997. The TH1/TH2 paradigm. *Immunol. Today.* 18:263–266. doi:10.1016/S0167-5699(97)80019-9

Scott, P., and S.H. Kaufmann. 1991. The role of T-cell subsets and cytokines in the regulation of infection. *Immunol. Today.* 12:346–348. doi:10.1016/0167-5699(91)90063-Y

Smith, G.L., and M. Law. 2004. The exit of vaccinia virus from infected cells. *Virus Res.* 106:189–197. doi:10.1016/j.virusres.2004.08.015

Sokol, C.L., N.Q. Chu, S. Yu, S.A. Nish, T.M. Laufer, and R. Medzhitov. 2009. Basophils function as antigen-presenting cells for an allergen-induced T helper type 2 response. *Nat. Immunol.* 10:713–720. doi:10.1038/ni.1738

Sun, J., R. Madan, C.L. Karp, and T.J. Braciale. 2009. Effector T cells control lung inflammation during acute influenza virus infection by producing IL-10. *Nat. Med.* 15:277–284. doi:10.1038/nm.1929

van der Klooster, J.M., L.A. Nurmohamed, and N.A. van Kaam. 2004. Bronchocentric granulomatosis associated with influenza-A virus infection. *Respiration.* 71:412–416. doi:10.1159/000079649

Wareing, M.D., A.B. Lyon, B. Lu, C. Gerard, and S.R. Sarawar. 2004. Chemokine expression during the development and resolution of a pulmonary leukocyte response to influenza A virus infection in mice. *J. Leukoc. Biol.* 76:886–895. doi:10.1189/jlb.1203644

Yamamoto, M., J.L. Vancott, N. Okahashi, M. Marinaro, H. Kiyono, K. Fujihashi, R.J. Jackson, S.N. Chatfield, H. Bluethmann, and J.R. McGhee. 1996. The role of Th1 and Th2 cells for mucosal IgA responses. *Ann. NY Acad. Sci.* 778:64–71. doi:10.1111/j.1749-6632.1996.tb21115.x

Yoneyama, H., K. Matsuno, and K. Matsushimaa. 2005. Migration of dendritic cells. *Int. J. Hematol.* 81:204–207. doi:10.1532/IJH97.04164

Yoon, H., K.L. Legge, S.S. Sung, and T.J. Braciale. 2007. Sequential activation of CD8+ T cells in the draining lymph nodes in response to pulmonary virus infection. *J. Immunol.* 179:391–399.

Zheng, W., and R.A. Flavell. 1997. The transcription factor GATA-3 is necessary and sufficient for Th2 cytokine gene expression in CD4 T cells. *Cell.* 89:587–596. doi:10.1016/S0092-8674(00)80240-8

Ziegler, S.F., and Y.J. Liu. 2006. Thymic stromal lymphopoietin in normal and pathogenic T cell development and function. *Nat. Immunol.* 7:709–714. doi:10.1038/ni1360